https://doi.org/10.5194/hess-2024-73
Preprint. Discussion started: 4 April 2024

Hydrology and Earth System Sciences
Open Access
EGU
Discussions

Relative importance of uncertain model parameters driving water fluxes in a Land Surface Model

David Luttenauer[1], Aronne Dell'Oca[2], Alberto Guadagnini[2], Sylvain Weill[1], Philippe Ackerer[1]

[1] Institut Terre et Environnement de Strasbourg, Université de Strasbourg, CNRS, ENGEES, F-67000 STRASBOURG, France

[2] Dipartimento di Ingegneria Civile e Ambientale, Politecnico di Milano, Milano, Italy

Corresponding author: Philippe Ackerer, ackerer@unistra.fr

Abstract

We focus on the way temporal distributions of key components of the water cycle are influenced by typically uncertain parameters embedded in a Land Surface Model. We rest on a joint analysis of multiple global sensitivity metrics to provide a comprehensive assessment of the ranking of the relative importance of uncertain factors of various origins on the hydrological system response. The latter is rendered in terms of the temporal dynamics of transpiration, evaporation, and groundwater recharge. The NIHM (Normally Integrated Hydrological Model) modular Land Surface model is applied to simulate realistic field conditions (in terms of, e.g., climate, vegetation, and soil type) associated with two watersheds in the Vosges region (France) across a one-year period. These watersheds are characterized by similar climatic conditions while being associated with differing soil types and vegetation. Uncertain model parameters we consider comprise monthly values of albedo and leaf area index, vegetation-related parameters, as well as parameters related to the soil types associated with the litter layer and root zone. Four diverse sensitivity indices are used to quantify impacts of uncertain model parameters on the whole probability distribution or given statistical moments of the density

https://doi.org/10.5194/hess-2024-73
Preprint. Discussion started: 4 April 2024

function of model outputs. Our results document that the strength of the relative importance of model parameters depends on the statistical moment considered. Evaporation is directly influenced by the energy flow through the canopy and by the parameters associated with the top litter layer. As one could expect, transpiration appears as mainly influenced by the vegetation characteristics and by albedo that influences the incoming radiation. Groundwater recharge is influenced only by a very limited number of model parameters. It mainly depends on soil-related parameters and is unexpectedly not sensible to any of the vegetation parameters considered, except the root layer thickness and the intercept.

https://doi.org/10.5194/hess-2024-73
Preprint. Discussion started: 4 April 2024

Hydrology and Earth System Sciences Discussions

1 Introduction

Since the work of Manabe (1969), Land Surface Models (LSMs) have become critical tools for modeling energy balance, water cycle, vegetation dynamics, and their feedbacks. They constitute one of the key routines employed in General Circulation Models (GCMs) to evaluate the effects of climate change on the Earth surface as well as in modeling workflows routinely used for water resources management. Numerous LSMs have been developed in the last decades (e.g. Blyth et al., 2020; Fisher and Koven, 2020; Overgaard et al., 2006; and references therein). These are characterized by various levels of complexity such as, e.g., LSMs described in Niu et al., (2011), Maneta and Silverman (2013), Decharme et al., (2019), Lawrence et al., (2019), Wiltshire et al., (2019) or Yokohata et al. (2019).

A primary purpose of a LSM is to simulate exchanges of energy and water between the land surface, the underground, and the atmosphere. Due to the variety of processes that are mathematically rendered therein, LSMs embed numerous input parameters related to vegetation, energy transfer and water fluxes across the atmosphere and in the soil. Many of these parameters (e.g., soil attributes or vegetation characteristics) are difficult to quantify through direct measurements and may vary across scales and locations. These elements typically lead to uncertainty in our knowledge of the values of such parameters (Beven and Smith, 2014). In case a target model output is not (or only minimally) affected by the particular value associated with certain parameters, it may be appropriate to rely on typical literature values for these. It is then important to properly identify parameters that significantly impact model outputs.

In this context, sensitivity analysis enables one to quantitatively rank the influence that diverse uncertain model parameters, involved in the mathematical rendering of different processes, have onto model predictions of interest. Thus, sensitivity analysis should be considered as an integral and essential step in the diagnosis and understanding of complex models of hydrological systems (Ferretti et al., 2016; Song et al., 2015; Vemuri et al., 1969; Razavi et al., 2021). Sensitivity analyses can yield

https://doi.org/10.5194/hess-2024-73
Preprint. Discussion started: 4 April 2024

Hydrology and Earth System Sciences
Open Access
Discussions

valuable information about LSMs development, potentially simplifying mathematical representations, and streamline LSMs calibration by omitting uninfluential parameters (Mc Cuen, 1973).

Demarty et al. (2005) perform a sensitivity analysis of soil heat conduction flux, sensible heat flux, latent heat flux, water content of the upper five soil centimeters and local directional brightness temperature considering 35 input parameters associated with the physically-based model SiSPAT-RS (Braud et al., 1995). Their findings indicate the saturated water content of the upper 5 cm of soil and the thermal infrared brightness temperature as the most influent model parameters. Liang and Guo (2003) compare the sensitivity of evapotranspiration, total runoff, sensible heat flux and soil moisture to 5 model parameters that appear in 10 different LSMs. Their results show that parameters associated with soil properties appear to play a more significant role than those associated with vegetation properties whereas the outputs of the diverse models considered exhibit the highest sensitivity to the maximum soil moisture content, considering three different hydroclimatic scenarios. Bastidas et al. (2006) assess parameter sensitivity of 5 different LSMs with increasing level of complexity in the description of vegetation-related physical processes. They show that (*a*) the sensitivity of the energy budget component to parameters with similar physical meaning employed in the diverse LSMs analyzed depends on the specific LSM model and varies depending on the location of the system, and (*b*) soil-related parameters could be considered as most influential. Based on the hydrologic model WetSpa (Wang et al., 1996), Yang et al. (2012) highlight the intense sensitivity of runoff flow rate of two water catchments to the parameters involved in the description of the evapotranspiration process. Li et al. (2013) employ diverse sensitivity analysis methodologies to assess the sensitivity of 6 model outputs of the LSM CoLM (Dai et al., 2003), i.e., sensible heat, latent heat, upward longwave radiation, net radiation, soil temperature, and soil moisture, with respect to 40 uncertain model parameters. Their results highlight that all model outputs are sensitive to the Clapp and Hornberger parameter (which is related to soil water retention, see Clapp and Hornberger, 1978), while (*i*) aerodynamic roughness length markedly influences the sensible and latent heat fluxes (along with the upward longwave and

https://doi.org/10.5194/hess-2024-73
Preprint. Discussion started: 4 April 2024

net radiations and soil temperature), and (*ii*) soil porosity chiefly governs soil moisture. Li et al. (2013) suggest that latent heat flux (related to evapotranspiration) is also sensitive to quantum efficiency of vegetation photosynthesis and minimum soil suction. Baroni and Tarantola (2014) employ classical variance-based Sobol indices to rank the importance of model parameters and forcing terms involved in the simulation of the mean soil moisture of the root zone, the cumulative evaporation, and the water flux below the root zone upon leveraging on the SWAP model (van Dam et al., 2008). Their results suggest uncertainty related to the crop parameters (i.e., crop height, root depth, and the Leaf Area Index (*LAI*)) does not have a significant effect on these three model outputs in the setting analyzed. Sobol indices estimated through a surrogate model are also used by Maina et al. (2022) to highlight the significant impacts of hydrodynamic parameters' uncertainties on simulated evapotranspiration. These Authors show that, under energy limited conditions and where plants have access to groundwater, the uncertainty on evapotranspiration is related to uncertainties in saturated hydraulic conductivities. Under water limited conditions, the parameters that contributes to the evaporation uncertainty are those related to unsaturated flow conditions.

While the above-mentioned studies constitute only a sample across the broad literature associated with diagnosis of LSMs through sensitivity analyses, they clearly show that the importance of model parameters depends on several factors (such as, e.g., the target model output considered, the processes embedded in the employed LSM, and the hydroclimatic conditions) and possibly on the selected sensitivity analysis methodology.

This work aims at providing a comprehensive sensitivity analysis across spatial and temporal locations within a hydrological system to highlight the most relevant model parameters and the corresponding processes that need to be considered in a LSM. Here, we rely on a modular LSM developed at the Institut Terre et Environment de Strasbourg (ITES – Strasbourg Earth and Environment Institute) to simulate key components of the water cycle (i.e., transpiration, evaporation, and groundwater recharge) and to assess their sensitivity with respect to diverse model parameters that are typically

https://doi.org/10.5194/hess-2024-73
Preprint. Discussion started: 4 April 2024

uncertain. We conduct a detailed sensitivity analysis by considering four diverse sensitivity indices: (*i*) the distribution-based Borgonovo index (Borgonovo et al., 2007); (*ii*) the variance-based Sobol indices (Sobol, 2001); and (*iii*) the moment-based *AMAE* and *AMAV* indices (Dell'Oca et al., 2017). The joint use of these metrics is exemplified upon relying on realistic field conditions (in terms of, e.g., climate, vegetation, and soil type) associated with two watersheds in the Vosges region (France) across a one-year period. The relevance of relying on various sensitivity analysis, each providing a unique contribution to enriching our knowledge of the system behavior, is underlined in several studies (e.g., Maina and Guadagnini, 2018; Bianchi Janetti et al., 2019; Ju et al., 2021; Sandoval et al., 2022; and references therein).

The methodological aspects associated with the LSM development and implementation, the definition of the various sensitivity indices, and the description of the hydrological settings associated with the catchments are presented in Section 2. Modeling results and the ensuing sensitivity analyses are illustrated in Section 3, while conclusions are drawn in Section 4.

2 Methodology

2.1 NIHM modular Land Surface Model

The NIHM (Normally Integrated Hydrological Model) modular Land Surface model (NIHM-MLSM, see Pan et al. (2015) and Jeannot et al. (2018)) is a numerical model design to compute on an hourly basis (*i*) the energy balance at the soil and vegetation (vegetation being considered as a single layer) surfaces, as well as, (*ii*) the water balance from the top of the vegetation layer to the groundwater table. Diverse mathematical formulations for processes such as transpiration, evaporation and snow melt, can be selected in conjunction with a modular structure on the basis of the observation that (*a*) application of a unique model formulation across different soil and vegetation types is questionable (Hogue et al., 2006) and (*b*) this allows adaptation to system complexity (Fisher and Koven, 2020).

https://doi.org/10.5194/hess-2024-73
Preprint. Discussion started: 4 April 2024

Hydrology and Earth System Sciences
Open Access
Discussions

Details of NIHM-MLSM are provided in the supplementary material. Here, we recall only the main mathematical formulations, assumptions and parametrization.

2.1.1 Energy balance

The different components of the energy balance for the surface near the canopy layer are:

$$\begin{cases} R_n = R_{S\downarrow}(1-\alpha_c)\left(1-e^{-K_{ext}LAI}\right)+\varepsilon_c R_{L\downarrow}-\varepsilon_c\zeta T_c^4 \\ H = \dfrac{\rho_a c_a}{r_{ac}}\left(T_c - T_a\right) \\ \rho_w \lambda Tr = \dfrac{\rho_a c_a}{\gamma(r_{ac}+r_c)}\left[e_s^{sat}\left(T_c\right)-e_s\right] \end{cases} . \quad (1)$$

The corresponding components for the soil surface are:

$$\begin{cases} R_{n,s} = R_{S\downarrow}(1-\alpha_s)e^{-K_{ext}LAI}+\varepsilon_s R_{L\downarrow}-\varepsilon_s\zeta T_s^4 \\ G = \dfrac{\rho_a c_a}{r_g}\left(T_s - T_g\right) \\ H = \dfrac{\rho_a c_a}{r_{as}}\left(T_s - T_a\right) \\ \rho_w \lambda E = \dfrac{\rho_a c_a}{\gamma r_{as}}\left(e_s^{sat}(T_s)-e_s\right) \end{cases} . \quad (2)$$

Here, R_n [W.m^{-2}] is net radiation at the surface; $\rho_w\lambda E$ and $\rho_w\lambda Tr$ [W.m^{-2}] are surface latent heat flux related to evaporation and transpiration, respectively; H [W.m^{-2}] represents sensible heat flux (also termed conductive heat flux) between the surface and the atmosphere; G [W.m^{-2}] is the conductive heat flux between the soil surface and the underground; $R_{S\downarrow}$ [W.m^{-2}] and $R_{L\downarrow}$ [W.m^{-2}] are the incoming solar radiation and the longwave radiation, respectively; α_s is the soil albedo (-); K_{ext} is the canopy attenuation coefficient [-]; LAI is the leaf area index [-]; ε_s is soil emissivity [-]; ζ is the

https://doi.org/10.5194/hess-2024-73
Preprint. Discussion started: 4 April 2024

Boltzman constant [W/m/K^4]; T_a, T_g, and T_S are the air, underground and soil temperature [K], respectively; ρ_w and ρ_a are water and air density [kg/m^3] respectively; c_a is the specific heat of dry air at constant pressure [J/kg/K]; r_g and r_{as} are the aerodynamic resistance at the soil and canopy surface, respectively [s/m]; e_s and e_s^{sat} are the water vapor pressure and the water vapor pressure at saturation [Pa], respectively; γ is the psychrometric constant [Pa/K]; and λ is the latent heat of water vaporization [J/Kg].

Main assumptions related to the formulation of the energy balance comprise the following:

- steady-state is considered, upon assuming that vegetation and soil layers have negligible heat capacity;
- conductive heat fluxes are expressed on the basis of a resistance analogy, similar to Ohm's law;
- the amount of energy absorbed by the vegetation and received by the ground are estimated by assuming a Beer-Lambert transmission reflectivity through the vegetation (Deardorff, 1978; Taconet et al., 1986) and depend on the leaf area index (*LAI*) and an attenuation coefficient (hereafter denoted as K_{ext});
- transpiration takes place only in the canopy; stomatal conductance is evaluated using a Jarvis-type multiplicative model (Cox et al., 1998; Jarvis, 1976) and is affected by the environmental factors embedded in the efficiency functions (solar radiation, air temperature, vapor pressure deficit); the *LAI* is used to scale stomatal conductance to canopy conductance;
- water intercepted by the canopy is assumed to evaporate with negligible impact on energy balance (Kergoat, 1998);
- the soil heat flux is approximated as proportional to the net radiation (Clothier et al., 1986; Choudhury and Monteith, 1988; Kustas and Daughtry, 1990); for this study, the coefficient of proportionality between the former and the latter is set at 0.5 γ (Singh and Sharma, 2017, Norman et al., 1995; Anderson et al., 1997; Boegh et al., 2000).

https://doi.org/10.5194/hess-2024-73
Preprint. Discussion started: 4 April 2024

The equations governing energy mass balance are solved upon considering the surface temperature as unknown and using a Newton Raphson method. If convergence is not reached after a maximum number of user-defined iterations, temperature is set to corresponding value associated with the previous time step. This approximation is assumed to be appropriate due to the small time steps employed (hourly time steps).

2.1.2 Water flow and balance

Water balance is formulated for three diverse compartments, i.e., the canopy, the snow cover, and the soil. Key concepts associated with the water balance model for the canopy are: (*i*) water from precipitation is partly stored in the canopy, whose storage capacity is limited to a maximum value; (*ii*) the intercepted water is subject to evaporation and does not contribute to throughfall (i.e., the process according to which excess water leaves wet leaves to reach the ground surface).

The snow model is adapted from the snow module of the HBV hydrological model (Seibert and Bergström, 2022; Seibert and Vis, 2012). It consists in splitting precipitation (after interception) in either snow, rain, or both. A conceptual model based on snowpack temperature is used to estimate snowmelt fluxes (Neitsch et al., 2002).

Flow in the unsaturated zone is described by introducing three types of reservoirs (or layers): (*i*) the litter, corresponding to the layer in contact with the atmosphere and where only evaporation takes place; (*ii*) the root zone, which is colonized by plant roots and supplies water for transpiration; and (*iii*) a set of sequential reservoirs to mimic vertical water movement below the root zone down to the groundwater table. Each reservoir is defined through a given water content at saturation, the water content at wilting point (which is also considered as the residual water content), and water content at field capacity.

Water from throughfall and melted snow infiltrates in the litter layer. Evaporation (as computed by energy balance at the soil surface) occurs only in this layer, and the amount of evaporated water is linearly related to water content. Water drained from the litter layer enters the root layer. Transpiration

https://doi.org/10.5194/hess-2024-73
Preprint. Discussion started: 4 April 2024

(estimated with the energy balance for the canopy) takes place only in this layer, and its amount is adapted according to the available water therein. Drainage from the different layers is estimated in two ways: (*i*) the water volume above the layer field capacity is drained immediately to the next layer, to represent water movement due to gravity; and (*ii*) when water content lies between the field capacity and the wilting point (i.e., residual water content), drainage is computed as an exponential function of the available water amount.

Similar to other LSMs, NIHM-LSM requires the estimation of numerous forcing terms and parameters related to climatic conditions, vegetation and soil characteristics. Several factors limit our ability to obtain a reliable estimate of these forcing terms and parameters. These include, e.g., incompatibility between the model scale and the support volume of the measurement and the inherent space and time variability of most of the parameters that makes the exhaustive knowledge of model parameters and forcing terms as practically unfeasible. Therefore, identification of the parameters that can be considered as most *important* to given model outputs is critical to effectively assist modeling and estimation of land surface energy and water fluxes. Note that we consider as *important* (or influential) those model parameters whose variations impact to some extent model outputs of interest, i.e., transpiration, evaporation and groundwater recharge fluxes in this study.

Such parameters are identified through a global sensitivity analysis in an *ab initio* context, i.e., the degree of uncertainty assigned to the vegetation and soil model parameters is grounded on a priori qualitative knowledges (e.g., prior experience, literature data). In the present study, we do not evaluate parameter uncertainty based on a model calibration procedure against experimental data associated with the modeled system (e.g., measured transpiration fluxes).

2.2 Global Sensitivity analysis

A critical step in diagnosing and understanding the functioning of a model works involves quantifying the relevance that different uncertain model parameters exert on the model results of interest to identify

https://doi.org/10.5194/hess-2024-73
Preprint. Discussion started: 4 April 2024

the (possible) influential and non-influential parameter sets. These are here assessed through global sensitivity analysis. In broad terms, the latter enables one to quantify the (relative) strength of the influence of the variability/uncertainty in a given parameter on the corresponding variability/uncertainty in the output(s) of the model analyzed.

Here, we rely on two complementary global sensitivity analysis methodologies: (*i*) density function- and (*ii*) and moment-based strategies. While the former is tailored to analyze the effects that variations of uncertain model parameters have on the whole (probability or cumulative) density function of the model output, the latter focuses on the impact on given statistical moments of the density function of model output. Here, we consider the Borgonovo index (Borgonovo et al., 2007) as a density function-based metric. For moment-based metrics, we use the Sobol indices (Sobol, 2001) and the *AMAE* and *AMAV* indices (Dell'Oca et al., 2017).

Considering $\boldsymbol{X}$ as a set of random independent parameters and Y as the corresponding model output, the Borgonovo index (B) associated with parameter X_i is defined as:

$$B_{X_i} = \frac{1}{2} \int f_{X_i}(x_i) \left[\int \left| f_Y(y) - f_{Y|X_i}(y) \right| dy \right] dx_i \tag{3}$$

Here, $f_{X_i}(x_i)$ is the marginal probability density function (pdf) of the *i*-th model (input) parameter X_i; $f_Y(y)$ and $f_{Y|X_i}(y)$ are the unconditional and conditional (to a given value of X_i) marginal pdf of Y, respectively. Note that the Borgonovo index grounds the concept of the sensitivity of Y to X_i on the base of the (average) distance between the unconditional pdf of the output and its counterparts stemming from conditioning on diverse plausible values of X_i. This index ranges in the unit interval, where a null value corresponds to scenario in which the pdf of Y is unaffected by variations in parameter X_i.

https://doi.org/10.5194/hess-2024-73
Preprint. Discussion started: 4 April 2024

Hydrology and Earth System Sciences Discussions

We also rely on the classical Sobol indices (Sobol, 2001) to quantify the contribution of the uncertainty in X_i to the model output variance when considered alone, *i.e.*, principal index SP_{X_i}, or as it interacts with other parameters, i.e., total index ST_{X_i}. The principal Sobol index associated with X_i is given by:

$$SP_{X_i} = \frac{V\left[E\left[y \mid X_i\right]\right]}{V\left[y\right]} \tag{4}$$

where E[-] and V[-] denote the expectation and variance operators, respectively, and $E[y|X_i]$ is the expected value of Y conditional to a particular value of X_i. The principal Sobol index measures the relative contribution of X_i to the model output variance without considering interactions with other uncertain model parameters. The corresponding total Sobol index embeds also the contributions of interactions with the remaining model parameters and is defined as:

$$ST_{X_i} = SP_{X_i} + \sum_{x_j} SP_{X_i,X_j} + \sum_{x_j,x_k} SP_{X_i,X_j,X_k} + \ldots \tag{5}$$

where SP_{X_i,X_j} is the fraction of model output variance due to the interactions between parameters X_i and X_j (the remaining symbols being characterized by a corresponding meaning). We recall that the total Sobol index represents the expected contribution of X_i to the variance of the model output, including contributions caused by its interactions with other input variables. Sobol indices are broadly used because of their simplicity and intuitive nature to assess sensitivity of models to input parameters by decomposing the total variance of a model output of interest into different contributions, each associated with a subset of parameters. These indices are used to measure the importance of individual parameters and interactions between parameters (Sobol, 2001).

To complement our investigation, we evaluate the moment-based metric introduced by Dell'Oca et al. (2017), termed *AMA* indices. The latter quantify sensitivity as the degree of variations in given statistical moments of the target model output Y that are due to the variability in model parameter X_i. Considering the expected value of Y, we introduce the following moment-based index:

$$AMAE_{X_i} = \begin{cases} E\left[\left|y_0 - E\left[y \mid X_i\right]\right|\right] / \left|y_0\right| & y_0 \neq 0 \\ E\left[\left|E\left[y \mid X_i\right]\right|\right] & y_0 = 0 \end{cases} \tag{6}$$

where y_0 is the unconditional expected value of Y. Considering the second (centred) statistical moment, i.e., the variance of Y, we introduce following index:

$$AMAV_{X_i} = E\left[\left|V[y] - V\left[y \mid X_i\right]\right|\right] / V[y] \tag{7}$$

Relying on the *AMA* indices enables one to assess the sensitivity of Y in terms of various salient features of the probability density function of the target model output, as rendered through diverse statistical moments. Here, we focus on the mean and the variance of the model output. These metrics have been applied in diverse settings, including scenarios related to, e.g., groundwater hydrology (Bianchi Janetti et al., 2019; Dell'Oca, 2023), subsurface energy resources associated with gas flow migration across low-permeability media (Sandoval et al., 2022), analysis of seismic metabarriers (Zeighami et al., 2023), dynamics of emerging contaminants in groundwater (Ceresa et al., 2023), or assessment of infiltration structures (Dell'Oca et al., 2023).

Our reliance on various sensitivity indices is in line with the observation that it is often difficult for one method to provide a complete sensitivity assessment. This is even more critical for complex hydrological systems of the kind we consider here (Mai et al., 2022).

https://doi.org/10.5194/hess-2024-73
Preprint. Discussion started: 4 April 2024

2.3 Study catchments and data-sets

The NIHM-MLSM model is run under realistic field conditions (in terms of climate, vegetation, and soil type) on two catchments in the Vosges region of northeastern France (i.e., in the Bruche and Doller catchments) that are characterized by similar climatic conditions while being associated with differing soil types and vegetation. While the model is run in a distributed way on the whole extent of each catchment, results are only illustrated for a selected location (or computational pixel) for each catchment, for simplicity. Selection of each of these pixels is based on the criterion that they are considered as a representative of the conditions associated with the corresponding catchment in terms of soil type, climate, and vegetation cover. Both locations are subject to an oceanic climate, being affected by continental traits (Peel et al., 2007) due to the action of Foehn. Consequently, considerable fluctuations in local climatic variables, such as air temperature or rainfall rates, are experienced. Historical streamflow data indicate a low-water period taking place between June and October and a high-water period between December and March (Banque HYDRO, 2020).

The first exemplary location considered in this study is located in the Bruche catchment, which is characterized only by vineyards on Calcosol soil. The second location considered is representative of the Doller catchment, which is covered by deciduous forest, moorland and heathland in combination with the Alocrisols soil. Figure 1 and 2 depict records of the main climatic forcings monitored across the study period, i.e., precipitation, temperature, wind speed, and solar radiation reaching the canopy for the Bruche and Doller watersheds, respectively.

https://doi.org/10.5194/hess-2024-73
Preprint. Discussion started: 4 April 2024

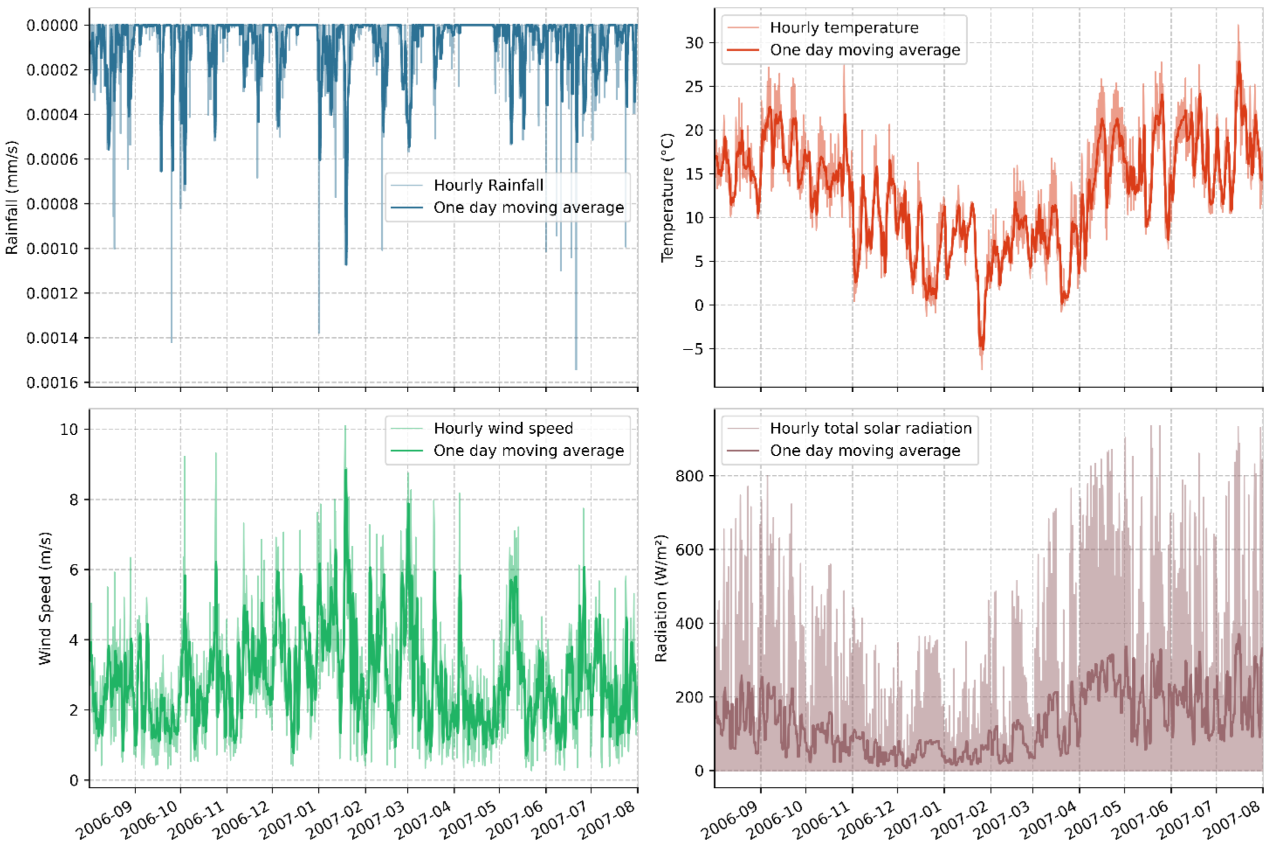

Figure 1: Main climatic forcing for the Bruche watershed.

https://doi.org/10.5194/hess-2024-73
Preprint. Discussion started: 4 April 2024

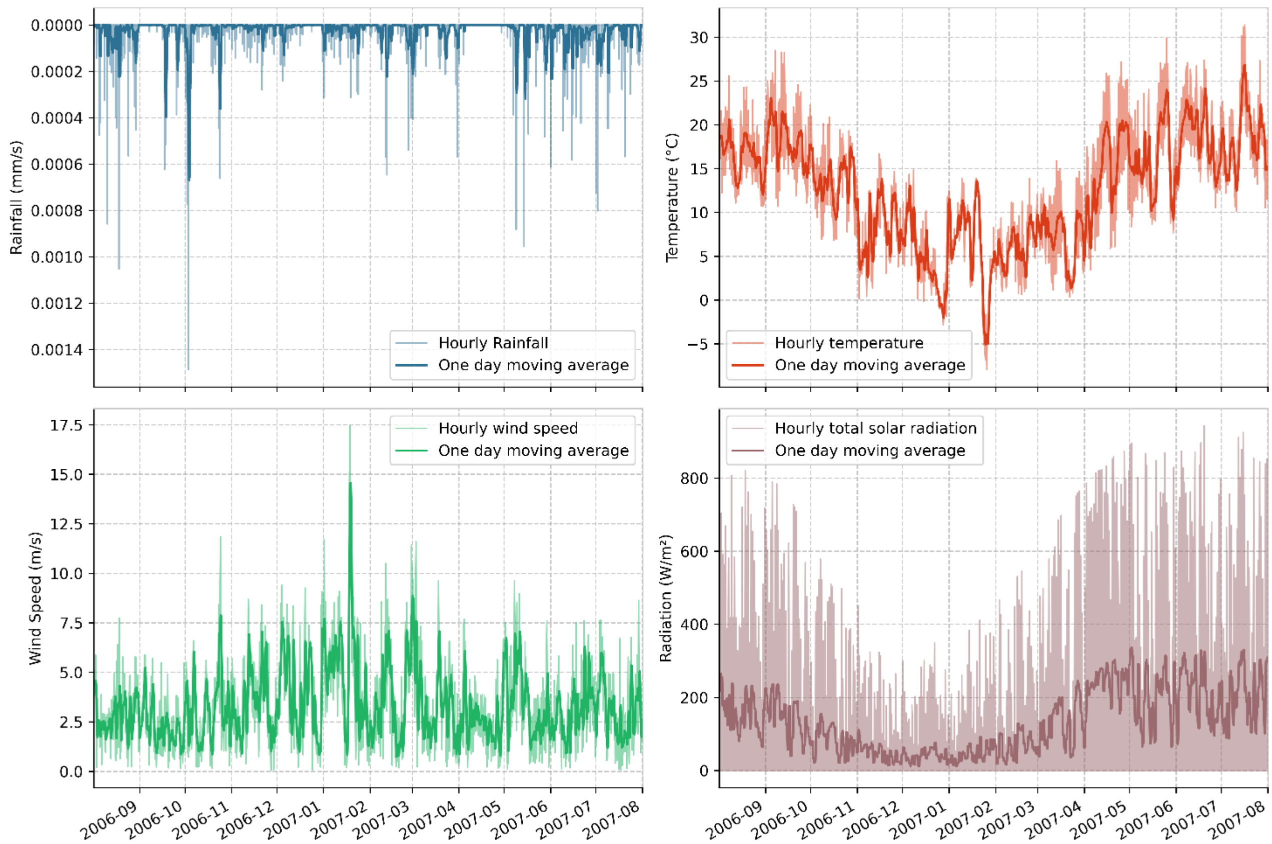

Figure 2: Main climatic forcing for the Doller watershed.

Climatic data (air temperature, air humidity, precipitation, snow, wind speed, incoming solar radiation, and longwave radiation) are included in the Safran database produced by Météo-France (Durand et al., 1993; Habets et al., 2008). The Safran system interpolates key climatic variables from ground measurements on a fixed grid of 8 × 8 km^2 with a hourly temporal resolution (Durand et al., 2009; Quintana-Seguí et al., 2008). It has been widely used to address hydrological monitoring and climate change studies (Vidal et al., 2010). Note that uncertainty on these forcing terms is not considered in this work which is otherwise specifically focused on the parameters required for LSMs.

https://doi.org/10.5194/hess-2024-73
Preprint. Discussion started: 4 April 2024

Hydrology and Earth System Sciences Discussions

In this study, the uncertain parameters involved in the evaluation of transpiration, evaporation, and groundwater recharge fluxes at a given time are:

- the *LAI* and the albedo; considering their smooth variation over time, we rely on linearly interpolated monthly data; this implies that a given simulation time is associated with two *LAI* and two albedo parameter values;
- five vegetation-related parameters per vegetation type (i.e., precipitation interception, radiation attenuation, root depth, stomatal conductance, and canopy height);
- five parameters for the litter layer (i.e., residual water content, field capacity, porosity, thickness, and drainage coefficient) and four parameters for the root layer (residual water content, field capacity, porosity, and drainage coefficient, root depth being considered as a vegetation dependent parameter) per soil type.

A total number of 18 parameters is associated with a given type of vegetation and a given type of soil.

Monthly values for *LAI* and albedo are estimated from satellite data at a spatial scale of 3×3 km^2 (downloaded from https://land.copernicus.eu/global/products/ (Copernicus Climate Change Service, 2018)). When several values are associated with a given month, we consider their average as a representative monthly value. If only one value is available, it is considered as the average value across the month. Albedo values for the vegetation are computed upon relying on the albedo value rendered by the satellite information and a prescribed albedo value for the soil assuming multireflection between the soil and the vegetation (see Supplementary Material (SM)). Parameter uncertainty is also provided in the dataset (in terms of a corresponding standard deviation).

The Corine Land Cover database (https://land.copernicus.eu/en/products/corine-land-cover) allows for the identification of distinct vegetation categories at each studied catchment at raster scale of 100m (European Union - SOeS, 2018). Table 1 lists the support (i.e., ranges of variability) associated with

https://doi.org/10.5194/hess-2024-73
Preprint. Discussion started: 4 April 2024

the uncertain vegetation-related parameters for the diverse vegetation types related to the two watersheds here considered. The width of these supports is identified on the basis of a detailed analysis of previous literature studies. For completeness, we list the main literature sources analyzed for each vegetation-related parameter:

- precipitation interception (Brecciaroli et al., 2012; Couturier and Ripley, 1973; Friesen and Van Stan, 2019; Kergoat, 1998; Nicholas et al., 2011);
- radiation attenuation coefficient (Zhang et al., 2014);
- root depths (Escamilla et al., 1991; Freeling and Walbot, 1994; Leuschner et al., 2001; Mueller et al., 2013; Richards, 2011; Grassland: Mission: Biomes, 2023);
- stomatal conductance (Gowdy et al., 2022; Brewer et al., 2022; Carter, 1998; Charreyron, 2011; Hovenden and Brodribb, 2000; Jonard et al., 2011; Juan Carlos Baca Cabrera, 2021; Kim and Verma, 1991; Mahhou et al., 2005; Mueller et al., 2013; Ocheltree et al., 2012; Reis and Ribeiro, 2020; Song et al., 2018; Tardieu et al., 1991; Winkel and Rambal, 1993; Zhang et al., 2012);
- canopy height (Campos et al., 2021; Liu et al., 2019; Matese et al., 2017; Grassland: Mission: Biomes, 2023; Peiffer et al., 2014; Smirnova et al., 2008).

Vegetation type	Interception [-]		Attenuation [-]		Root Depth [m]		Stomatal conductance [m/s]		Canopy height [m]	
T1	0.1	0.4	0.16	0.54	0.5	2.5	0.005	0.015	0.2	1.2

https://doi.org/10.5194/hess-2024-73
Preprint. Discussion started: 4 April 2024

T2	0.1	0.53	0.29	0.65	0.6	2.3	0.0002	0.0036	12.6	27.0
T3	0.14	0.22	0.35	0.65	0.2	1.0	0.0011	0.0110	0.2	2.1

Table 1: Vegetation-dependent parameters (minimum and maximum values) for **T1:** Vineyards (Bruche catchment), **T2:** Deciduous forests (Doller catchment) and **T3:** Grasslands, Natural grasslands and pastures, Moors and heathland (Doller catchment).

Only the vineyards vegetation is considered (T1 in Table 1) at the Bruche catchment. Two types of vegetation are considered for the exemplary location selected at the Doller catchment. These correspond to (*i*) vegetation composed mainly of broad-leaved species, including shrub and bush understoreys for 2/3 of the pixel area (T2 in Table 1) and (*ii*) vegetation resulting mainly from forest degradation (low and closed cover, dominated by bushes, shrubs and herbaceous plants) for 1/3 of the pixel area (T3 in Table 1).

Soil types are classified upon relying on the Regional Soil Reference System for Alsace and Vosges (https://data.europa.eu/data/datasets/fr-341142131-araa_bdsol-alsace_250000_2011?locale=fr). Six main categories are identified (Chambre Régionale d’Agriculture Grand Est, 2011, 2015) and denoted according to the World Reference Base for Soil Resources (IUSS Working Group WRB, 2022).In this work we consider only the first two soil layers (i.e., litter and root zone) and groundwater recharge is assumed to coincide with drainage from the root zone, the overall thickness of the unsaturated zone being limited to a few meters. Table 2 lists ranges of variability associated with the uncertain soil-related parameters for the diverse soil types of interest. As stated above, the width of these supports is set on the basis of previous studies (Belfort et al., 2018; Clapp and Hornberger, 1978; Dingman, 2002). Note that soil types S1 and S2 constitute typical traits of the Bruche and Doller catchment, respectively.

Soil Type	**Root layer**		**Litter layer**		
	Field capacity θ_c	**Porosity** θ_s	**Field capacity** θ_c	**Porosity** θ_s	**Thickness (m)**

https://doi.org/10.5194/hess-2024-73
Preprint. Discussion started: 4 April 2024

S1	0.22	0.33	0.42	0.48	0.25	0.35	0.50	0.80	0.05	0.15
S2	0.12	0.16	0.40	0.45	0.17	0.25	0.50	0.80	0.05	0.15

Table 2: Soil-dependent parameters (minimum and maximum values) for **S1:** Calcosols and Calcisols (Bruche catchment) and **S2:** Alocrisols (Doller catchment).

Drainage coefficients for both layers and all soil types are set to range between 1.0×10^{-7} and 9.0×10^{-7}. This range of variability has been defined on the basis of the temporal pattern of groundwater recharge fluxes obtained through preliminary model runs (details not shown). Residual water content is fixed at 0.01 for all soil types.

Evaluation of the global sensitivity indices listed in Section 2.2 is performed through a numerical Monte Carlo (MC) approach. Parameter values are randomly sampled by considering model parameters as independent and identically distributed random variables, each characterized through a uniform distribution with support given in Table 1 and 2. With reference to *LAI* and albedo, the semi-width of the support is set to the value of the standard deviation provided in the Copernicus data sets.

Sobol indices are calculated upon considering the algorithm described in Saltelli (2007). A total of 147,500 and 168,000 simulations are performed for the Bruche and the Doller catchment, respectively. The number of simulations is higher for the Doller catchment due to the additional vegetation type (see Table 1).

The temporal window associated with our simulations spans a period of two years (01/09/2005 to 31/08/2007). The analyses target solely the second year of simulations, to minimize impacts of initial conditions on model outputs.

https://doi.org/10.5194/hess-2024-73
Preprint. Discussion started: 4 April 2024

3 Results

3.1 Catchments behaviors

Here, we illustrate the type of results obtained with the modeling study to assist grasping the overall behavior of the systems and to provide a first quantitative appraisal of the nature of the available observations and modeling outputs related to the complex hydrological systems analyzed. We rely on graphical depictions rendered in terms of the expected value +/- one standard deviation of daily averaged values grounded on the set of MC simulations for the period from August 1st, 2006 to July 31th, 2007. Temporal dynamics of actual evaporation, actual transpiration, and groundwater recharge fluxes are provided in Figures 3 and 4 for the selected locations in the two watersheds (see Section 2.3), together with the corresponding observed rainfall series. Detailed quantitative results concerning the main components of the water cycle are listed in Table 3 and 4 for the Bruche and Doller catchment, respectively.

	Autumn	**Winter**	**Spring**	**Summer**	**Total**
Precipitation (mm)	212.7	165.1	237.7	287.6	903.2
(%)	*24*	*18*	*26*	*32*	*100*
Evaporation (mm)	39.21 / 4.41	54.93 / 6.30	65.50 / 12.73	60.70 / 15.52	220.34 / 33.98
(%)	*18*	*25*	*30*	*28*	*100*
Transpiration (mm)	10.74 / 4.21	2.05 / 1.59	55.85 / 18.69	60.25 / 18.69	128.89 / 40.84
(%)	*8*	*2*	*43*	*47*	*100*
Groundwater Recharge (mm)	116.65 / 25.31	75.00 / 7.98	63.12 / 11.95	74.86 / 24.03	329.62 / 60.88
(%)	*35*	*23*	*19*	*23*	*100*

Table 3. Amount of water volume (in mm) for the different seasons and over the year for the Bruche catchment. Values of transpiration, evaporation, and groundwater recharge are evaluated through the NIHM-MLSM model (mean / standard deviation). Percentage values (%) are defined as the ratio between seasonal values and their yearly counterparts.

	Autumn	**Winter**	**Spring**	**Summer**	**Total**
Precipitation (mm)	566.4	780.03	414.54	780.63	2541.3
(%)	*22*	*31*	*16*	*32*	*100*
Evaporation (mm)	34.45 / 1.52	71.22 / 3.63	43.17 / 8.47	25.69 / 2.53	174.54 / 13.71
(%)	*20*	*41*	*25*	*15*	*100*
Transpiration (mm)	15.4 / 4.06	1.60 / 0.71	44.22 / 12.63	58.64 / 14.2	119.86 / 30.21
(%)	*13*	*1*	*37*	*49*	*100*
Groundwater Recharge (mm)	315.19 / 80.72	609.40 / 24.83	201.77 / 35.9	246.20 / 105.8	1372.56 / 236.23
(%)	*23*	*44*	*15*	*18*	*100*

Table 4. Amount of water volume (in mm) for the different seasons and over the year for the Doller catchment. Values of transpiration, evaporation, and groundwater recharge are evaluated through the NIHM-MLSM model (mean / standard deviation). Percentage values (%) are defined as the ratio between seasonal values and their yearly counterparts.

https://doi.org/10.5194/hess-2024-73
Preprint. Discussion started: 4 April 2024

Hydrology and Earth System Sciences
Open Access
Discussions

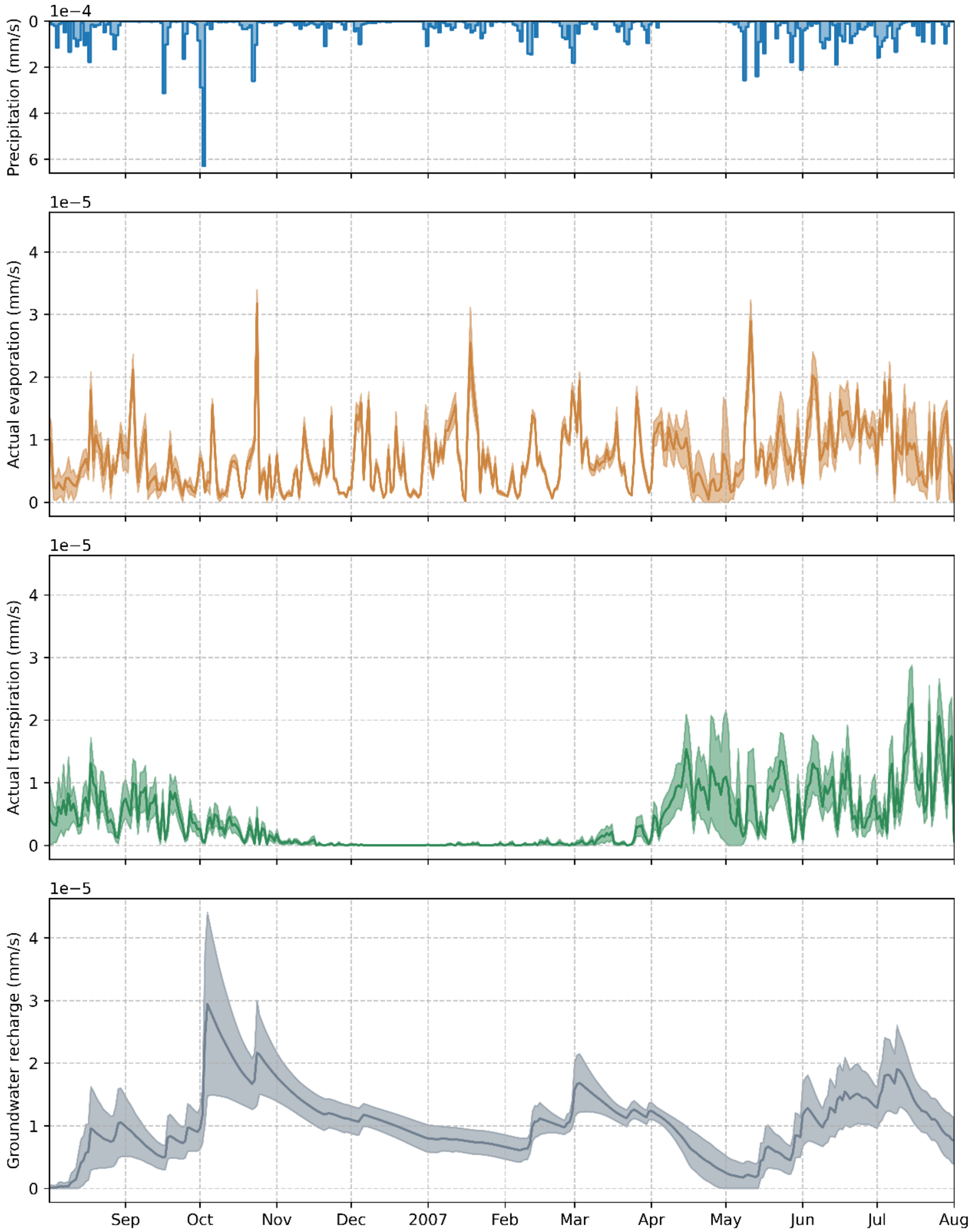

Figure 3 Observed (a) precipitation, (b) calculated evaporation and (c) transpiration together with (c) groundwater recharge at the Bruche watershed.

https://doi.org/10.5194/hess-2024-73
Preprint. Discussion started: 4 April 2024

Hydrology and Earth System Sciences Discussions

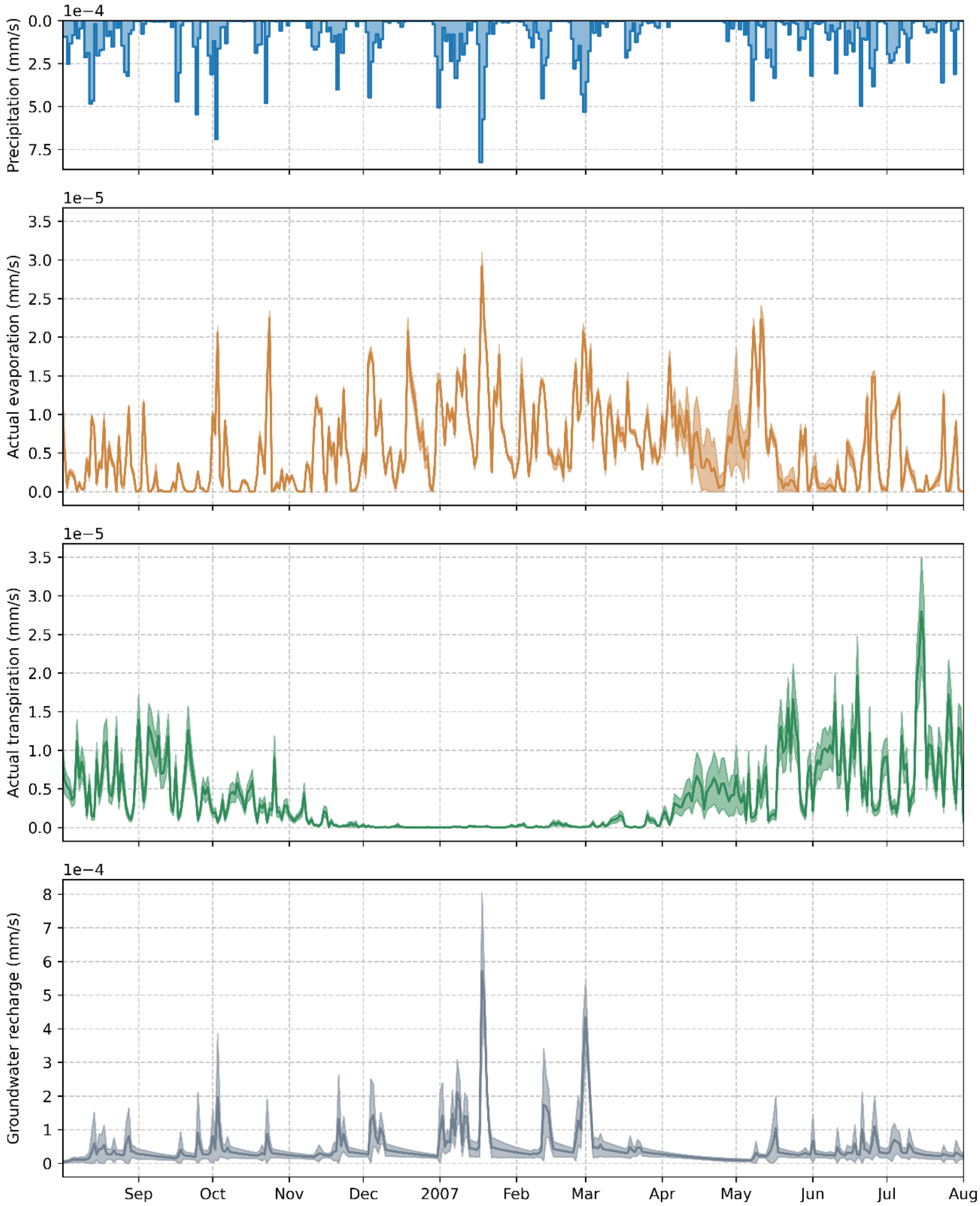

Figure 4. Observed (a) precipitation, (b) calculated evaporation and (c) transpiration together with (c) groundwater recharge at the Doller watershed (note the different scale for recharge

https://doi.org/10.5194/hess-2024-73
Preprint. Discussion started: 4 April 2024

Despite the geographical proximity of the watersheds, precipitation patterns are quite different. Tables 3-4 indicate that the annual amount of precipitated water over the year is very different between the two catchments (903.2 mm for the Bruche and 2541.3 mm for the Doller) and that during Winter the Bruche catchment is relatively dry, while the Doller catchment experiences significant precipitation events. These findings are further corroborated by the inspection of Fig.s 3a, 4a.

Tables 3-4 suggest that evaporation in both catchments occurs over the whole year, with very similar total amount of evaporated water. However, inspection of Figs. 3b, 4b and of the seasonal values listed in Table 3-4, reveals that evaporation intensify during Winter for the Doller catchment, due to more frequent and intense precipitation (in line with the previous observation regarding the difference in the precipitation patterns during Winter). Additionally, despite the stronger similarity in the precipitation patterns during Summer (see also percentage values in Table 3-4) evaporation at the Doller catchment appears to be less pronounced than at Bruche. We attribute this difference to the (overall) lower values of the attenuation coefficient (characteristic of vineyard vegetation cover) at Bruche with respect to the counterparts at Doller (see Table 1). The periods with the highest uncertainties in the evaporation (as quantified in terms of standard deviation of model outputs) are generally observed to take place between rainy episodes (at both catchments) and during Summer at Bruche, when a significant amount of solar radiation is intercepted by the vineyard that is characterize by a more uncertain attenuation coefficient that the vegetation covers present at Doller (see Table 1).
Joint inspection of Tables 3-4 and Figs. 3c and 4c highlights that transpiration fluxes at both catchments are characterized by a typical seasonal variability, with very poor transpiration fluxes in Winter (less than 2% of the annual transpired water) and increased transpiration (close to 50%) in Summer. These findings are in line with the weather conditions (temperature, radiation) and vegetation status. When active, transpiration is more intense in the Bruche watershed due to its higher soil storage capacity that allows for water extraction in the root zone to fulfil the evaporation potential. Notably,

https://doi.org/10.5194/hess-2024-73
Preprint. Discussion started: 4 April 2024

Hydrology and Earth System Sciences Discussions
Open Access

uncertainty in the transpiration is larger in correspondence of the growing phase of vegetation during Spring at both watersheds.

Comparison of Tables 3-4 reveals different (relative) amounts of groundwater recharge at the two watersheds: groundwater recharge represents about 36% and 54% of the yearly precipitation for the Bruche and Doller catchment, respectively. We mainly ascribe these differences to the diverse values of the soil field capacity (see Table 2) at the two catchments (recall that the amount of water above field capacity constitutes the groundwater recharge at a given time step). Such element also implies very different patterns (see Fig.s 3d, 4d) in the behavior of the groundwater recharge at the two catchments: the higher values of the Bruche soil field capacity result in smoother temporal fluctuations of the groundwater recharge, while the lower values of the field capacity for the Doller catchment yield a higher reactivity. At the same time, groundwater recharge mostly occurs during autumn and Winter at both catchments while still remaining significant also during Summer (around 20% of the annual recharge). Notably, in both catchments the uncertainty in the groundwater recharge tends to increase with the expected value of the latter.

The results from the Monte Carlo simulations can also be analyzed in terms of the ensuing pdf of an output of interest at a given time. Figure 5 depicts exemplary pdfs obtained for diverse model outputs, i.e., (a) evaporation, (b) transpiration, (c) groundwater recharge at Bruche, (d) groundwater recharge at Doller, at different times, considering unconditional results (red curves) and conditioning on diverse subintervals of variability for a given parameter. With reference to the latter element, we select here five equiprobable subintervals, for (a) litter drainage, (b) albedo coefficient, (c) root drainage rate and (d) root depth. This type of visual analysis is akin to a regionalized sensitivity analysis. It helps one to grasp the impact that conditioning on diverse values (comprised within subintervals according to which the overall support is partitioned) of a parameter might have on the pdf of an output of interest.

https://doi.org/10.5194/hess-2024-73
Preprint. Discussion started: 4 April 2024

Hydrology and Earth System Sciences
Open Access
EGU
Discussions

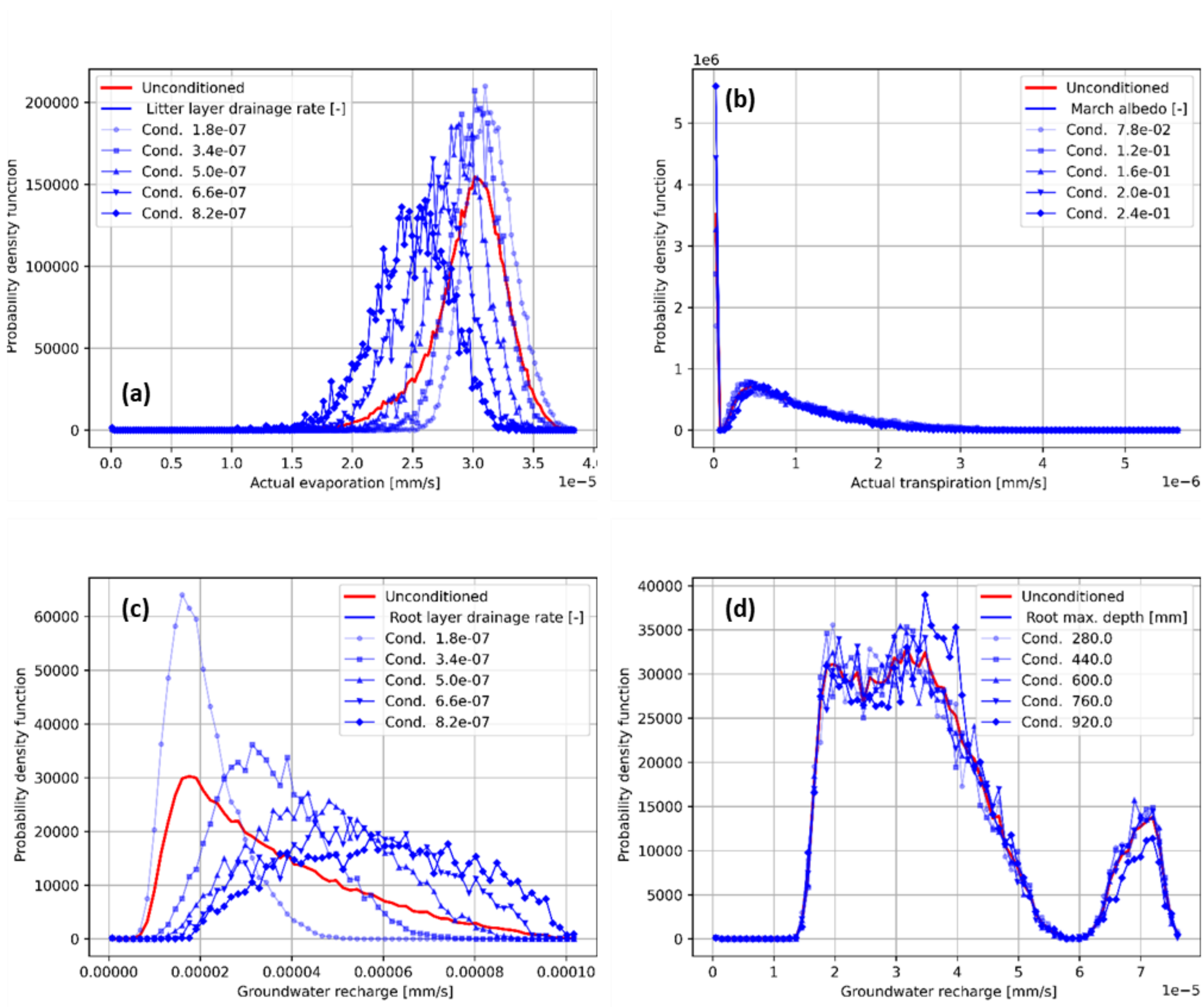

Figure 5. Probability density functions related to: (a) evaporation on July 7th, 4 p.m. at Bruche with prescribed litter drainage rate; (b) transpiration on December 31th, 12 a.m. at Bruche with prescribed albedo coefficients; (c) groundwater recharge on October 5th, 12 a.m. at Bruche with prescribed root drainage rate(d) groundwater recharge on February, 2nd, 12 a.m. at Doller with prescribed root depth. In each panel, we consider the unconditional (red curve) pdf of each output and its counterparts

conditioned (blue curves) on five different (equally probable) subintervals (middle bin conditioning (denoted as Cond.) value provided in the legend) according to which the support of a given parameter is partitioned.

Inspection of Figure 5 reveals several interesting features. The pdfs of the actual evaporation rate, as recorded on September 7th at 4.00 p.m. at Bruche, visually resemble a Gaussian distribution (with a slight asymmetry) and conditioning on smaller litter drainage values results in lower average evaporation rates and higher variance (see Fig. 5a). Null values of the actual transpiration rate are generally likely to occur during the December 31th at 12 a.m. at Bruche, while greater values of the albedo coefficient lead to higher average and variance (see Fig. 5b). Inspection of the pdfs of the groundwater recharge, as recorded on May 10th at 12.00 a.m. at Bruche (Fig. 5c), suggests a strong sensitivity to the root drainage coefficient. On the other hand, the pdf of the groundwater recharge, as recorded on February 11th at 12.00 a.m. at Doller, exhibits a bimodal behavior and appears to be insensitive to the root depth (Fig. 5d).

These preliminary investigations for the diverse outputs and their response to model parameter variations suggest a complex behavior of the LSM here investigated. A quantitative appraisal of sensitivity is illustrated in Section 3.2 on the basis of the metrics introduced in Section 2.2.

3.2 Global Sensitivity Analysis.

We compute the global sensitivity indices introduced in Section 2.2 on an hourly basis over a temporal window of one year. Figure 6 depicts color-coded (from red/high to white/low) values of *B* (Eq. 3) *ST* (Eq. 5), *AMAE* (Eq. 6), and *AMAV* (Eq. 7) indices for the evaporation rate at Bruche across the year and the diverse model parameters (listed along the vertical axis; corresponding parameter identification number is defined in the Symbol List of the Supplementary Material). Figure 7 depicts corresponding results for the Doller catchment. Fig.s 8-11 are patterned after Fig.s 6-7 considering the results for transpiration rate and groundwater recharge.

We recall that, B (similar to all other indices) should vanish for certain outputs of interest that one knows are for sure insensitive to certain parameters. For example, the value of B for the evaporation at Bruche during the month of July associated with the *LAI* of January must be zero. However, inspection of Fig. 6a does not reflect this anticipated outcome. This apparent anomaly is attributed to a random noise (that would require a markedly high amount of additional computation hours to be reduced) stemming from the still incomplete sampling of the parameters space (despite our analysis incorporates an extensive number of random samples). Drawing from these findings, we identify a threshold value of $B = 0.17$ (average value in correspondence of instances associated with an expected null value of B) as a benchmark for evaluating the adequacy of parameter sampling within our sensitivity analysis. Consequently, we disregard from our sensitivity analysis instances in which B falls below 0.17, i.e., we assign a value of zero to *B*, *ST*, *AMAV*, and *AMAE* to enhance interpretability of visual representations.

Overall, the evaporation rate in the two catchments (see Fig.s 6 and 7) is mainly sensitive to the characteristics of the litter layer (in terms of layer thickness, field capacity, and drainage rate), the amount of radiation reaching the soil surface (as expressed through the attenuation coefficient), and the *LAI*. The relative influence of parameters related to the litter layer is generally higher for the variance (see *ST*, *AMAV*) than for the expected value (see *AMAE*) of evaporation in both catchments. Additionally, if a parameter influences the expected value of the evaporation rate at a given period during the year, it also influences its variance (the opposite not being generally observed).

https://doi.org/10.5194/hess-2024-73
Preprint. Discussion started: 4 April 2024

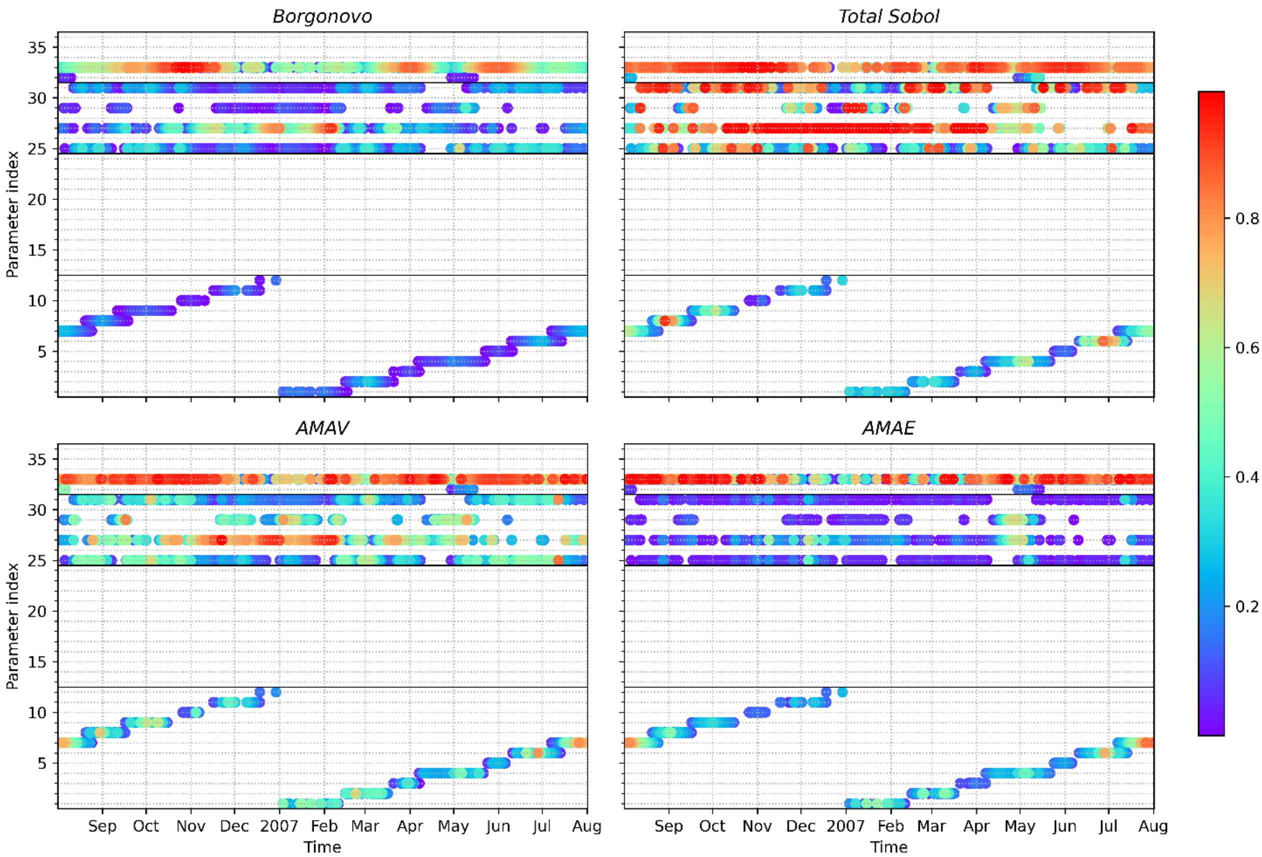

Figure 6. Temporal behavior of the sensitivity indices related to the evaporation rate at the Bruche catchment. Parameter id from 1 to 12 corresponds to *LAI*; parameter id = 25 denotes root layer field capacity, 27 is litter layer drainage coefficient, 29 is litter layer thickness, 31 is litter layer field capacity, and 33 is attenuation coefficient (see Supplementary Material for the complete list of parameter identifiers

Results for the indices associated with measurements of uncertainty of the output (i.e., *B*, *ST*, and *AMAV*) at the Bruche catchment suggest the uncertainty in the evaporation rates switches from being dominated by the litter layer drainage coefficient during Winter to being majorly influenced by the variability in attenuation coefficient of the vegetation during the rest of the year. Considering the sensitivity of the expected value of the evaporation rate (as rendered through *AMAE*), the attenuation

https://doi.org/10.5194/hess-2024-73
Preprint. Discussion started: 4 April 2024

coefficient of the vegetation is the predominant parameter across the year with the exception of the Winter season when the litter layer drainage coefficient gains relevance during a dry period in December (see Fig. 1a), while the *LAI* becomes influential during the subsequent more wet period in January. A similar pattern is documented also in correspondence of the dry month of April (here, also the litter layer thickness gains some importance), which is then followed by the wet month of May. Additionally, the *LAI* attains its highest influence (considering all of the sensitivity indices) during Summer (July-September).

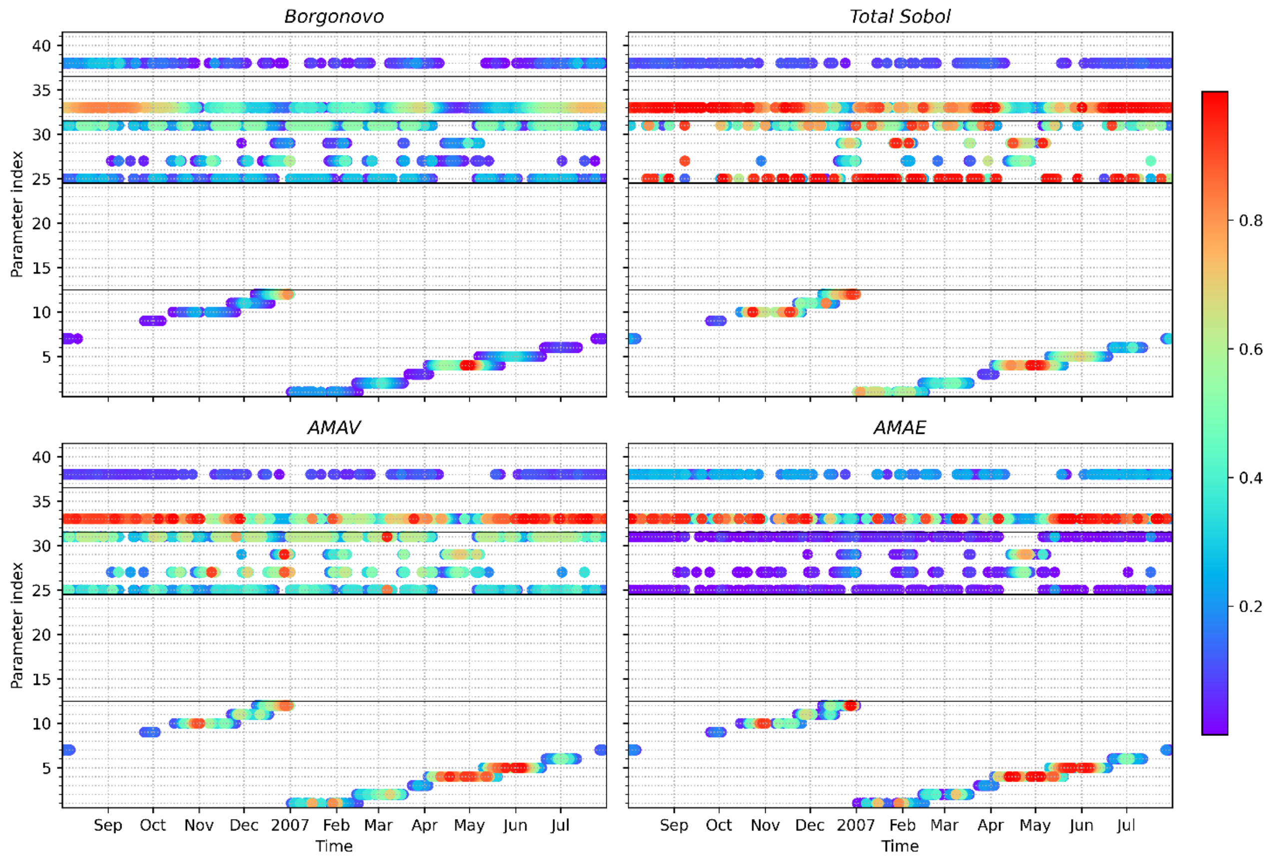

https://doi.org/10.5194/hess-2024-73
Preprint. Discussion started: 4 April 2024

Figure 7. Temporal behavior of the sensitivity indices related to evaporation at the Doller catchment. Parameter id from 1 to 12 correspond to *LAI*; parameter id = 25 corresponds to root layer field capacity, 27 is litter layer drainage coefficient, 29 is litter layer thickness, 31 is litter layer field capacity; parameter id = 33 and 38 correspond to the attenuation coefficient for the two types of vegetation (see Supplementary Material for the complete list of parameter identifiers

With reference to the Doller catchment, the attenuation coefficient of the deciduous forest (T2 in Table 2) has a strong influence over the uncertainty (i.e., *B* , *ST*, and *AMAV*) and the expected value (i.e., *AMAE*) of the transpiration rate, the dry periods during December and April being an exception. Note that values of the corresponding indices for the other vegetation type (T3 in Table 2) shows a reduced influence because it corresponds to only 1/3 of the land cover. At the same time, the soil layer parameters that are most consistently influential to uncertainty of the evaporation rate across the year are the litter and root layer field capacities, while they appear not to influence the expected value of the evaporation rate at Doller. The drainage rate and thickness of the litter gain relevance only during the no-rain period in April, jointly with the *LAI*, whereas the attenuation coefficient of deciduous forest (T2 in Table 2) displays a reduced relevance. In contrast to Bruche, *LAI* is here mostly relevant during October to June while being less relevant during Summer. Our results suggest that field capacity of the litter and root layers are more relevant in the Doller than their counterparts in the Bruche watershed. At the same time, the litter drainage coefficient is overall less relevant in Doller than in Bruche. Similar to what we observe at Bruche, the litter field capacity is not influential when the rainy period starts (i.e., in May).

With reference to transpiration (Fig.s 8 and 9), our results show that parameters related to vegetation are characterized by a relative importance of that is significantly higher than their counterparts related to soil. The relative influence of some parameters is sometimes higher when focusing on the expected value of the transpiration rate than it is for its variance (compare *AMAE* to corresponding values of *ST*

https://doi.org/10.5194/hess-2024-73
Preprint. Discussion started: 4 April 2024

Hydrology and Earth System Sciences
Discussions

and *AMAV*). This is clearly the case with the parameters that regulate the amount of energy reaching the canopy, especially in Summer for *LAI* and in Winter for albedo.

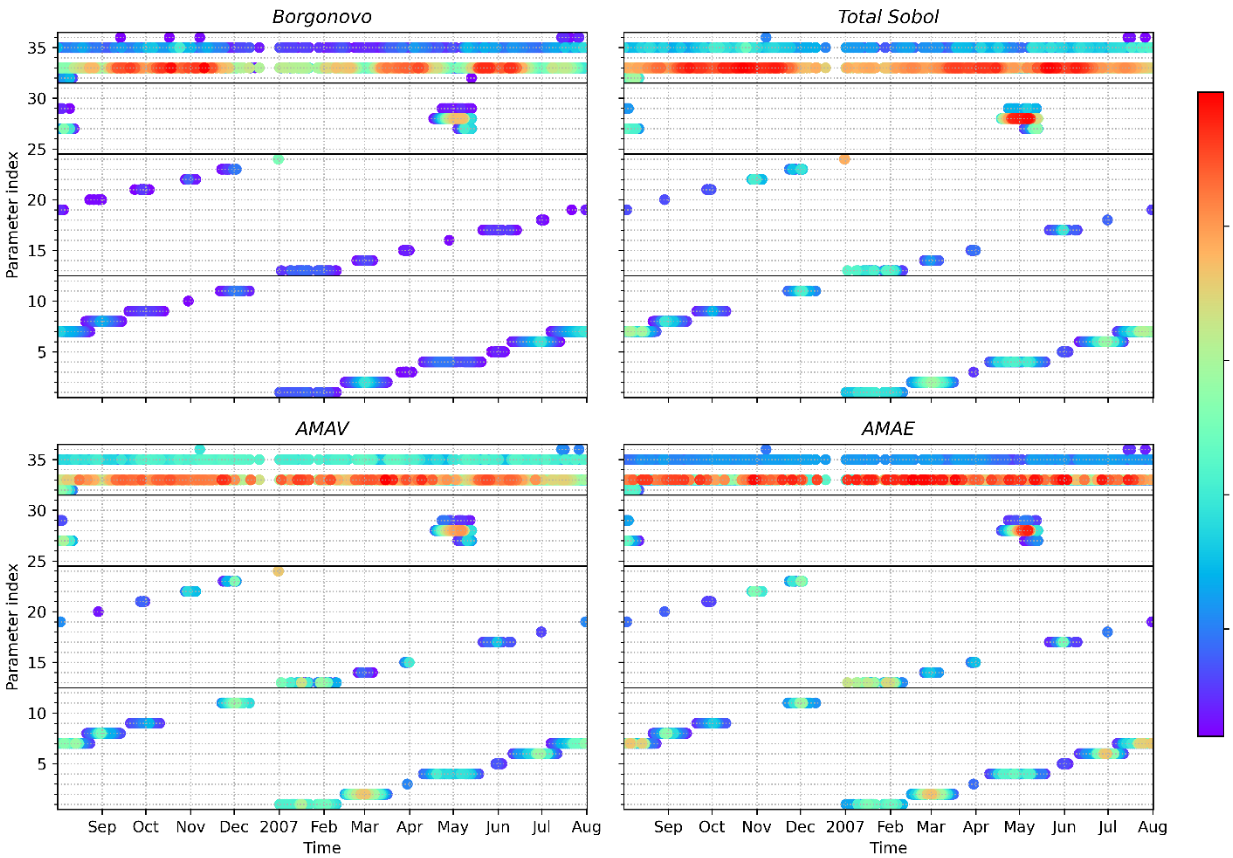

Figure 8. Temporal behavior of the sensitivity indices related to transpiration at the Bruche catchment. Parameter id from 1 to 12 correspond to *LAI*; parameter id from 13 to 24 correspond to albedo; parameter id = 33 and 35 correspond to the attenuation coefficient and to maximum stomatal conductance, respectively (see Supplementary Material for the complete list of parameter identifiers).

Inspection of Fig. 8 highlights that transpiration in the Bruche catchment is overall sensitive to vegetation-related parameters (chiefly to the attenuation coefficient and to stomatal conductance) during the year. Otherwise, the litter layer drainage coefficient exhibits a strong influence during the

https://doi.org/10.5194/hess-2024-73
Preprint. Discussion started: 4 April 2024

wet period in May that follows the no-rain period of April. The displayed sensitivity is consistent with the observation that water available in the root layer for transpiration is supplied by the litter layer, by drainage from the litter layer. At the same time, transpiration in Bruche exhibits a pattern of sensitivity to all of the parameters associated with *LAI* during the year in close similarity to what we observe for evaporation (see Fig. 6). Sensitivity to the albedo coefficient is mostly relevant during the Winter period where solar radiation is quite limited. Interestingly, the impact of the parameters related to the vegetation (attenuation coefficient and maximum stomatal conductance) on the expected value and variance of the transpiration rate are different. The attenuation coefficient mainly affects the expected value of transpiration (see corresponding values of *AMAE* in Fig. 8) as compared to its variance (see corresponding values of *TS* or *AMAV* in Fig. 8), whereas the relative importance of stomatal conductance is more marked for the variance than for the expected value.

https://doi.org/10.5194/hess-2024-73
Preprint. Discussion started: 4 April 2024

Hydrology and Earth System Sciences
Discussions

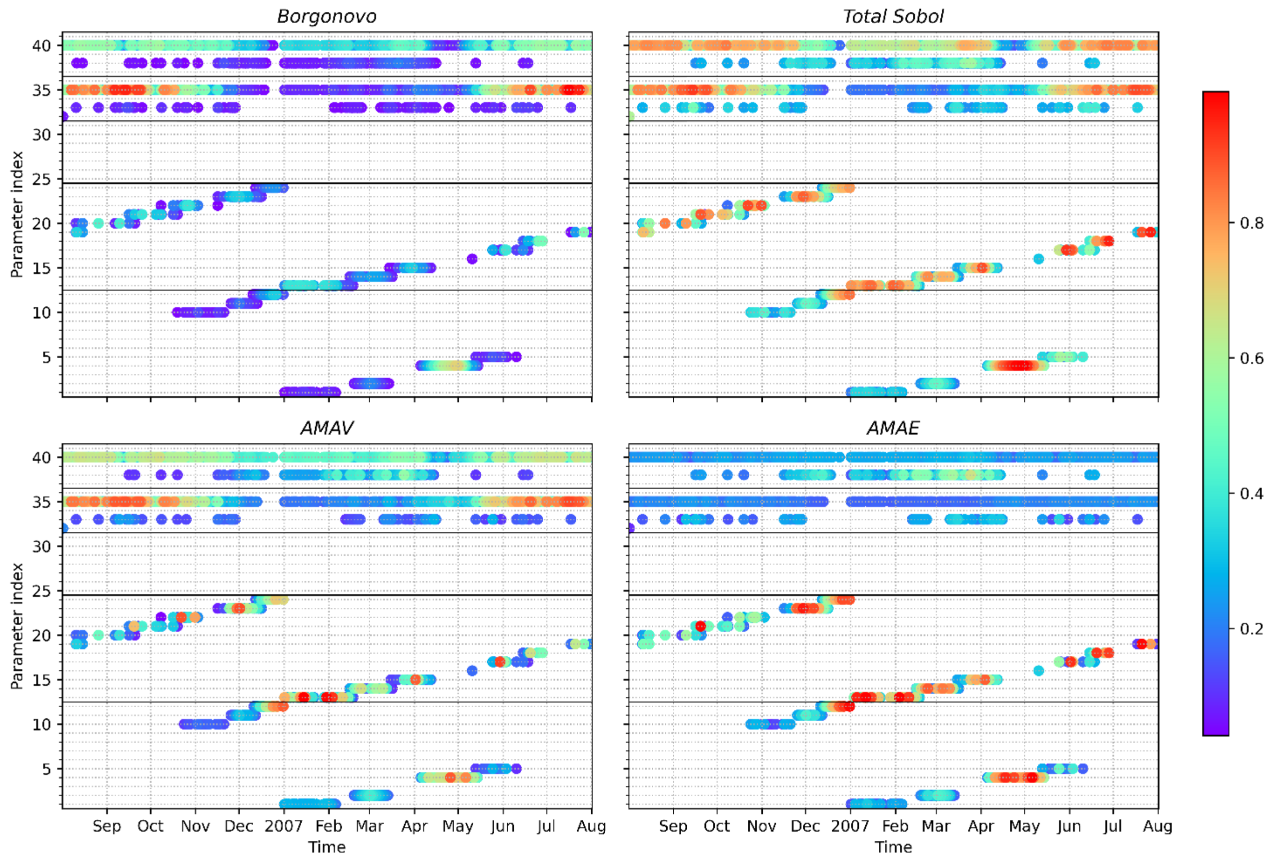

Figure 9. Temporal behavior of the sensitivity indices related to transpiration at the Doller catchment. Parameter id from 1 to 12 correspond to *LAI*; parameter id from 13 to 24 correspond to albedo; parameter id = 33 and 38 correspond to the attenuation coefficient of both vegetation types; parameter id = 35 and 40 correspond to maximum stomatal conductance of both vegetation types (see Supplementary Material for the complete list of parameter identifiers

Considering transpiration in the Doller catchment, Fig. 9 reveals that: (*i*) the *LAI* exerts a marked influence during the no-rain period of April and December (similar to the sensitivity of evaporation in Doller; see Fig. 7), while it is not influential during Summer; (*ii*) the albedo coefficient consistently impacts transpiration during the Winter-middle of Spring period (i.e., during low radiation periods) while the strength of its influence is more intermittent during the rest of the year; (*iii*) parameters

https://doi.org/10.5194/hess-2024-73
Preprint. Discussion started: 4 April 2024

Hydrology and Earth System Sciences
Discussions

related to the soil layer have no influence on transpiration in Doller during the whole year; (*iv*) during Winter, transpiration appears to be chiefly controlled by the albedo coefficient, the maximum stomatal coefficient and the attenuation coefficient of the deciduous forest; (*v*) in contrast to Bruche, the maximum stomatal conductance of the deciduous forests (T3 in Table 2) and of the degraded forest (T2 in Table 2), are the most relevant vegetation-related parameters in Doller (the former being especially relevant during Summer and fall, while the latter is more uniformly influential during the year). The variation in the sensitivity of the transpiration rate to vegetation-related parameters across the two catchments aligns with the distinct ranges of variability assigned to the stomatal conductance among different types of vegetation. Specifically, the stomatal conductance of the forest (that dominates at Doller) is relatively low as compared to that of vineyards (vegetation type of Bruche).

The results encapsulated in Figs. 10 and 11 surprisingly show that groundwater recharge is sensitive to very few parameters. None of the vegetation related parameters are ranked as important on the basis of the diverse sensitivity metrics here considered, intercept being the sole exception. Inspection of Fig. 10 highlights that groundwater recharge in the Bruche watershed can be considered as chiefly sensitive to the root drainage coefficient and, albeit to a reduced extent, to the rainfall interception. In particular, the root drainage coefficient is affecting the uncertainty in the groundwater recharge in Bruche in a consistent manner when considering B, ST and $AMAV$ (Fig. 10a-c). The same finding holds for the sensitivity of groundwater recharge to the rainfall intercept (see Fig. 10a-c; note the zero values during the no-rain period, as expected). Considering the expected value of groundwater recharge (see Fig. 10d), the root drainage coefficient shows a strong influence during the rain events of May (that follows the no-rain period of April), while rainfall interception is generally less influent on the expected value of the groundwater recharge during the whole year.

https://doi.org/10.5194/hess-2024-73
Preprint. Discussion started: 4 April 2024

Hydrology and Earth System Sciences
Discussions

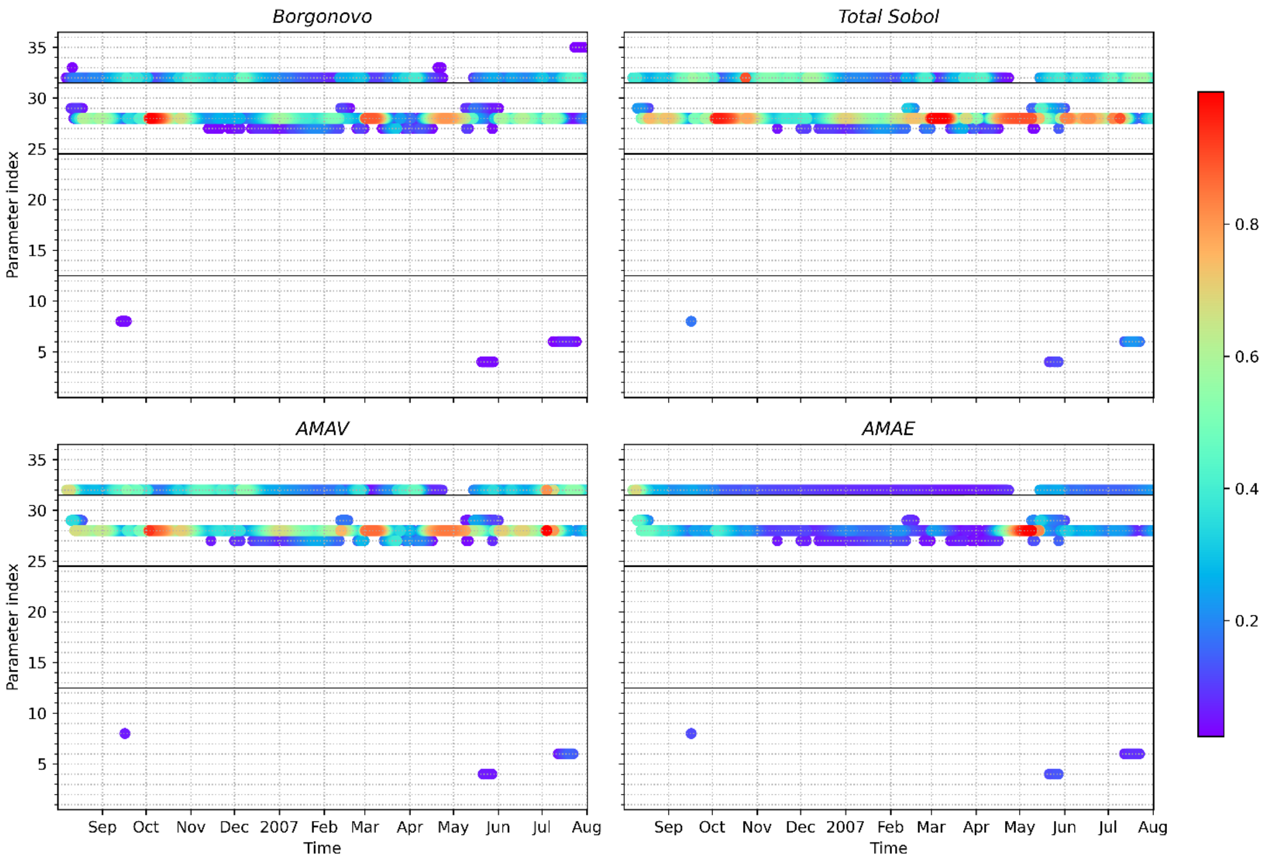

Figure 10. Temporal behavior of the sensitivity indices related to groundwater recharge at the Bruche catchment. Parameter id 28 and 32 correspond to root drainage coefficient and rainfall interception, respectively (see Supplementary Material for the complete list of parameter identifiers

https://doi.org/10.5194/hess-2024-73
Preprint. Discussion started: 4 April 2024

Hydrology and Earth System Sciences Discussions
Open Access
EGU

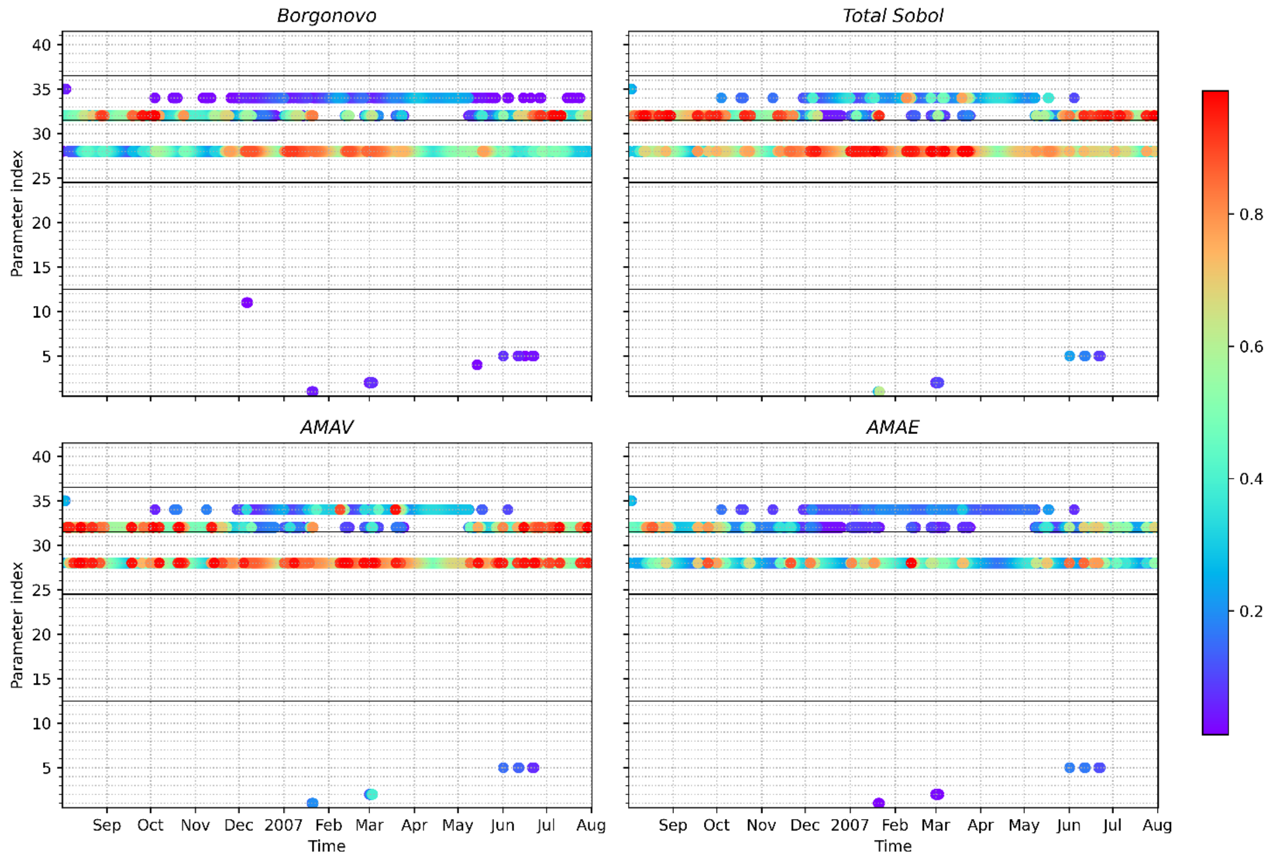

Figure 11. Temporal behavior of the sensitivity indices related to groundwater recharge at the Doller catchment. Parameter id 28, 32, and 34 correspond to root drainage coefficient, rainfall interception and root layer thickness, respectively (see Supplementary Material for the complete list of parameter identifiers.

Analysis of Fig. 11 highlights that groundwater recharge in the Doller is majorly sensitive to the root drainage coefficient and the rainfall interception. Rainfall interception by the canopy (T2 in Table 2) is dominant during Summer while the root zone drainage rate plays an enhanced role in Winter. This variability of parameter contributions to groundwater flux sensitivity is consistent with the amount of available water in the system across diverse seasons. In Summer, when soils are generally dry, small variations in the amount of water reaching the soils surface can trigger threshold effects that influence the amount of water transpired and evaporated and, therefore, the availability of water for groundwater recharge. Otherwise, in Winter, when soils are often quite wet, the rate of root zone drainage can have a major impact on the amount of water recharging the aquifer. During the latter period, a small degree of sensitivity is also recorded for the root zone layer thickness.

To summarize the key results of the sensitivity analysis conducted for the evaporation, transpiration, and groundwater recharge rates Table 5 lists for each model output the major sensitive parameters, identified by a '✓' sign.

		Vegetation				**Litter**			**Root**		
	Albedo	*LAI*	κ_p	K_{ext}	g_s^{max}	θ_c	T_L	κ_d	θ_c	T_L	κ_d
Evaporation		✓		✓		✓	✓	✓	✓		
Transpiration	✓	✓		✓	✓						
Groundwater recharge			✓							✓	✓

Table 5. Sensitivity of the target outputs of NIHM-LSM to uncertain input parameters (κ_p: rainfall interception; K_{ext}: radiation attenuation; g_s^{max}: maximum stomatal conductance; θ_c: field capacity; T_L: layer thickness; κ_d: drainage rate). Sensitive parameters are identified by a '✓' sign.

Most of the results summarized in Table 5 are intuitive, groundwater recharge being an exception. Evaporation only occurs in the top litter layer and is directly related to the energy flow through the canopy that then reaches ground surface. As one could expect, transpiration appears as mainly influenced by the vegetation characteristics and by albedo that influences the incoming radiation Surprisingly, groundwater recharge is not sensible to any vegetation parameters, except the root layer thickness and the intercept. This is possibly related to the observation that groundwater recharge appears only when precipitations are significant and/or when transpiration rates are very small due to a reduced energy (for example during Winter). When transpiration is significant, recharge to groundwater takes place solely after a period of precipitations that allows transpiration and replenishment of the water stored in the unsaturated zone.

4 Conclusion

We focus on the diagnosis of the behavior of the recently developed NIHM (Normally Integrated Hydrological Model) modular Land Surface model. The latter embeds a variety of critical hydrological processes and, similar to other land surface models, is characterized by a marked degree of parametrization. Temporal dynamics of water fluxes associated with transpiration, evaporation, and groundwater recharge are analyzed through global sensitivity analysis to discriminate the relative importance of uncertain model parameters. Uncertainty sources comprise incomplete knowledge of monthly values of albedo and leaf area index, as well as of parameters related to vegetation and soil types constituting the litter layer and root zone. As opposed to previous studies on sensitivity analyses of land surface models, we provide an assessment of various aspects of sensitivity upon considering a joint analysis of multiple GSA metrics. These enable us to quantify the relative importance of our knowledge of a given model parameter on sensitivity metrics associated with the whole probability distribution (Eq. 3) or the first two statistical moments (i.e., mean and variance; Eqs. 4, 6 and 7) of the density function of the target model outputs. Our analyses are exemplified through the simulation of realistic field settings characterizing two watersheds in the Vosges region (France) across a one-year period. Our study leads to the following major conclusions.

1. The strength of the relative importance of model parameters typically varies in time and depends on the statistical moment associated with the probability distribution of the model output of interest. For example, we document that the relative influence of parameters related to the litter layer is generally higher for the variance than for the expected value of evaporation

https://doi.org/10.5194/hess-2024-73
Preprint. Discussion started: 4 April 2024

in both catchments analyzed (Fig.s 6 and 7). The attenuation coefficient mainly affects the expected value of transpiration as compared to its variance (Fig. 8), the relative importance of stomatal conductance being more marked for the variance than for the average.

2. Water fluxes related to evaporation are chiefly influenced by the energy flow through the canopy and by the parameters characterizing the top litter layer. Transpiration appears to be mainly influenced by the vegetation characteristics and by albedo rather than by soil-related parameters, which play a very minor role. Groundwater recharge is influenced only by a very limited number of model parameters. Our result document that its mean and variance are mainly driven by the soil-related parameters, root layer thickness and intercept, while uncertainty in the remaining vegetation parameters is somehow unexpectedly not contributing to these. While most of these results can be intuitive, resting on rigorous GSA metrics yields an appropriate quantification of the relative strength of the way uncertainties related to model parameters propagates onto different statistical moments of the probability distribution of the modeled water fluxes. Since characteristics of the soils related to the litter layer and root zone play an important role in the evaluation of the evaporation and groundwater recharge fluxes, our results emphasize the need for targeted studies on modeling of flow across the soil component to best characterize these model outputs. Otherwise, the evaluation of these water fluxes would require a priori values for some vegetation-related parameters such as canopy height and stomatal conductance.
3. Relying on multiple sensitivity metrics, each focused on a given aspect of the uncertainty associated with a model response of interest, contributes to enhance our ability to quantify the relative importance of uncertainties linked to parameters of multiple origins. While a moment-independent analysis of the type linked to the distribution-based Borgonovo index may be subject to some operational constraints because of the need of assessing the complete probability density function of the model outcome of interest, it can nevertheless be employed as a measure of the overall impact of a model parameter on the probability distribution of the

https://doi.org/10.5194/hess-2024-73
Preprint. Discussion started: 4 April 2024

water fluxes considered. When coupled with prior knowledge of the system functioning (as for example in the case where some parameters are not involved in the computation of the water flux of interest), the results associated with this metric can be employed to gauge the quality of sampling of the model parameter space (see Section 3.2). The total Sobol indices and the *AMAV* indices provide very similar results in terms of ranking parameter importance with respect to water fluxes variance.

We recall that each land surface model implements various degrees of complexities for diverse processes. It is also recognized that uncertainty sources affecting land surface models typically comprise incomplete knowledge in (*a*) conceptual and mathematical formulation of models and processes therein and (*b*) parameters embedded in such models. As such, future research efforts will be aimed at extending our knowledge on the relative impact of uncertain processes (and their parameterization) on the different components of the water budget included in a land surface model.

https://doi.org/10.5194/hess-2024-73
Preprint. Discussion started: 4 April 2024

Code and data availability:
The code and data will be made available using a shared folder upon request.

Author contribution:
PA, AD, AG and SW designed the research; DL produced the data; all authors contributed to the analysis and interpretation of the results; DL and PA produced figures, tables and the first draft. All authors contributed to improve the manuscript. AG and PA wrote the submitted versions, using feedback from all the co-authors.

Competing interests:
The contact author has declared that none of the authors has any competing interests.
Some authors are members of the editorial board of HESS.

Acknowledgements
Daniel Luttenauer acknowledges support of the French Ministry of Agriculture and ENGEES for support through FCPR.
Alberto Guadagnini acknowledges the *Chaire Gutenberg* (Région Grand Est France, Strasbourg City and Strasbourg University).
Philippe Ackerer acknowledges support of the Politecnico di Milano (grant Senior Resident Researcher 2023).
Aronne Dell'Oca acknowledges support of the National Recovery and Resilience Plan (NRRP), Mission 4 Component 2 Investment 1.4 - Call for tender No. 3138 of December 16, 2021, rectified by Decree n.3175 of December 18, 2021 of Italian Ministry of University and Research funded by the European Union – NextGenerationEU; Project code CN_00000033, Concession Decree No. 1034 of June 17, 2022 adopted by the Italian Ministry of University and Research, CUP D43C22001250001, Project title "National Biodiversity Future Center - NBFC".

https://doi.org/10.5194/hess-2024-73
Preprint. Discussion started: 4 April 2024

References

Baca Cabrera, J.C., The key role of stomatal conductance in controlling the grassland vegetation response to a changing environment, Technische Universität München, 67 pp., 2021.

Banque HYDRO: http://www.hydro.eaufrance.fr/, last access: 4 February 2020.

Baroni, G., and Tarantola S., A General Probabilistic Framework for Uncertainty and Global Sensitivity Analysis of Deterministic Models: A Hydrological Case Study. Environmental Modelling & Software, 51, 26-34, https://doi.org/10.1016/j.envsoft.2013.09.022, 2013.

Bastidas, L. A., Hogue, T.S., Sorooshian, S., Gupta, H.V., and Shuttleworth, W. J., Parameter Sensitivity Analysis for Different Complexity Land Surface Models Using Multicriteria Methods. Journal of Geophysical Research: Atmospheres, 111, D20, https://doi.org/10.1029/2005JD006377, 2006.

Belfort, B., Toloni, I., Ackerer, P., Cotel, S., Viville, D., and Lehmann, F., Vadose Zone Modeling in a Small Forested Catchment: Impact of Water Pressure Head Sampling Frequency on 1D-Model Calibration, Geosciences, 8, 72, https://doi.org/10.3390/geosciences8020072, 2018.

Beven, K. J., and Smith, P. J., Concepts of information content and likelihood in parameter calibration for hydrological simulation models. ASCE J Hydrol Eng, doi: 10.1061/(ASCE)HE.1943-5584.0000991, 2014.

Boegh, E., Schelde, K., and Soegaard, H., Estimating Transpiration Rates in a Danish Agricultural Area Using Landsat Thermal Mapper Data, Physics and Chemistry of the Earth, Part B: Hydrology, Oceans and Atmosphere 25, 7-8, 685-689, https://doi.org/10.1016/S1464-1909(00)00085-X, 2000.

Bianchi Janetti, E., Guadagnini, L., Riva, M., and Guadagnini, A., Global sensitivity analyses of multiple conceptual models with uncertain parameters driving groundwater flow in a regional-scale sedimentary aquifer. Journal of Hydrology, 574, 544-556, https://doi.org/10.1016/j.jhydrol.2019.04.035, 2019.

Blyth, E.M., Arora, V.K., Clark, D.B., Dadson, S.J., De Kauwe, M.G., Lawrence, D.M., Melton, J.R., Pongratz, J., Turton, R.H., Yoshimura, K., and Yuan, H., Advances in Land Surface Modelling. Curr Clim Change Rep 7, 45–71. https://doi.org/10.1007/s40641-021-00171-5, 2021.

Borgonovo, E., A new uncertainty importance measure. Reliability Engineering & System Safety 92, 771–784. https://doi.org/10.1016/j.ress.2006.04.015, 2007.

Braud, I., Dantas-Antonino, A. C., Vauclin, M., Thony J.L., and Ruelle, P., A simple soil-plant-atmosphere transfer model (SiSPAT) development and field verification, J. Hydrol., 166, 213 – 250, 1995.

Brecciaroli, G., Cocco, S., Agnelli, A., Courchesne, F., and Corti, G., From rainfall to throughfall in a maritime vineyard, Sci. Total Environ., 438, 174–188, https://doi.org/10.1016/j.scitotenv.2012.08.044, 2012.

Brewer, K., Clulow, A., Sibanda, M., Gokool, S., Odindi, J., Mutanga, O., Naiken, V., Chimonyo, V. G. P., and Mabhaudhi, T., Estimation of Maize Foliar Temperature and Stomatal Conductance as Indicators of Water Stress Based on Optical and Thermal Imagery Acquired Using an Unmanned Aerial Vehicle (UAV) Platform, Drones, 6, 169, https://doi.org/10.3390/drones6070169, 2022.

Campos, J., García-Ruíz, F., and Gil, E., Assessment of Vineyard Canopy Characteristics from Vigour Maps Obtained Using UAV and Satellite Imagery, Sensors, 21, 2363, https://doi.org/10.3390/s21072363, 2021.

Carter, G. A., Reflectance Wavebands and Indices for Remote Estimation of Photosynthesis and Stomatal Conductance in Pine Canopies, Remote Sens. Environ., 63, 61–72, https://doi.org/10.1016/S0034-4257(97)00110-7, 1998.

Ceresa, L., Guadagnini, A., Rodríguez-Escales, P., Riva, M., Sanchez-Vila, X., and Porta, G. M., On Multi-Model assessment of complex degradation paths: The fate of diclofenac and its transformation products. Water Resources Research, 59, e2022WR033183. https://doi.org/10.1029/2022WR033183, 2023.

Chambre Régionale d'Agriculture Grand Est, Base de données du Référentiel Régional Pédologique d'Alsace : carte des pédopaysages d'Alsace à 1/250 000, en format DoneSol IGCS, 2011.

Chambre Régionale d'Agriculture Grand Est, Base de données du Référentiel Régional Pédologique de Lorraine : carte des pédopaysages de Lorraine à 1/250 000, en format DoneSol IGCS, 2015.

Charreyron, M., Suivi de la transpiration et de la conductance stomatique chez le pommier sous trois régimes hydriques : irrigation, sécheresse et réhydratation, Université Blaise Pascal (Clermont Ferrand 2) (UBP), FRA., 2011.

Choudhury, B. J. and Monteith, J. L., A four-layer model for the heat budget of homogeneous land surfaces, Q. J. R. Meteorol. Soc., 114, 373–398, https://doi.org/10.1002/qj.49711448006, 1988.

https://doi.org/10.5194/hess-2024-73
Preprint. Discussion started: 4 April 2024

Clapp, R. B., and Hornberger, G. M., Empirical equations for some soil hydraulic properties, Water Resour. Res., 14, 601–604, https://doi.org/10.1029/WR014i004p00601, 1978.

Clothier, B. E., Clawson, K. L., Pinter, P. J., Moran, M. S., Reginato, R. J., and Jackson, R. D., Estimation of soil heat flux from net radiation during the growth of alfalfa, Agric. For. Meteorol., 37, 319–329, https://doi.org/10.1016/0168-1923(86)90069-9, 1986.

Copernicus Climate Change Service, Leaf area index and fraction absorbed of photosynthetically active radiation 10-daily gridded data from 1981 to present, https://doi.org/10.24381/CDS.7E59B01A, 2018.

Couturier, D. E. and Ripley, E. A., Rainfall interception in mixed grass prairie, Can. J. Plant Sci., 53, 659–663, https://doi.org/10.4141/cjps73-130, 1973.

Cox, P. M., Huntingford, C., and Harding, R. J., A canopy conductance and photosynthesis model for use in a GCM land surface scheme, J. Hydrol., 212–213, 79–94, https://doi.org/10.1016/S0022-1694(98)00203-0, 1998.

Dai, Y., Zeng, X., Dickinson R.E., Baker, I., Bonan G.B., Bosilovich M.G., Denning A.S., Dirmeyer P.A., Houser P.R., Niu G., Oleson, K.W., Schlosser, A., and Yang ZL., The Common Land Model. Bulletin of the American Meteorological Society 84, 8: 1013-1024. https://doi.org/10.1175/BAMS-84-8-1013., 2003.

Deardorff, J. W., Efficient prediction of ground surface temperature and moisture, with inclusion of a layer of vegetation, J. Geophys. Res., 83, 1889, https://doi.org/10.1029/JC083iC04p01889, 1978.

Decharme, B., Boone, A., Delire, C., and Noilhan, J., Local Evaluation of the Interaction between Soil Biosphere Atmosphere Soil Multilayer Diffusion Scheme Using Four Pedotransfer Functions, Journal of Geophysical Research, 116, D20, D20126, https://doi.org/10.1029/2011JD016002, 2011.

Dell'Oca, A., Sensitivity analysis: an Operational picture. Water Resour. Res., 59, e2022WR033780. https:// doi.org/10.1029/2022WR033780, 2023.

Dell'Oca, A., Riva, M., Guadagnini, A., Moment-based metrics for global sensitivity analysis of hydrological systems. Hydrol. Earth Syst. Sci. 21, 6219–6234. https://doi.org/10.5194/hess-21-6219-2017, 2017.

Dell'Oca, A., Guadagnini, A., Riva, M., Probabilistic assessment of failure of infiltration structures under model and parametric uncertainty, Journal of Environmental Management, 344, 1-13, e2022WR033387, https://doi.org/10.1016/j.jenvman.2023.118466, 2003.

https://doi.org/10.5194/hess-2024-73
Preprint. Discussion started: 4 April 2024

Demarty, J., Ottle, C., Braud, I., Olioso, A., Frangi, JP., Gupta, H.V., and Bastidas, L.A., Constraining a Physically Based Soil-Vegetation-Atmosphere Transfer Model with Surface Water Content and Thermal Infrared Brightness Temperature Measurements Using a Multiobjective Approach. Water Resources Research 41, 1, https://doi.org/10.1029/2004WR003695, 2005.

Dingman, S. L., Physical hydrology, 2nd ed., Prentice Hall Upper Saddle River, N.J., Upper Saddle River, N.J., 2002.

Durand, Y., Brun, E., Merindol, L., Guyomarc'h, G., Lesaffre, B., and Martin, E., A meteorological estimation of relevant parameters for snow models, Ann. Glaciol., 18, 65–71, https://doi.org/10.3189/S0260305500011277, 1993.

Durand, Y., Giraud, G., Laternser, M., Etchevers, P., Mérindol, L., and Lesaffre, B., Reanalysis of 47 Years of Climate in the French Alps (1958–2005): Climatology and Trends for Snow Cover, J. Appl. Meteorol. Climatol., 48, 2487–2512, https://doi.org/10.1175/2009JAMC1810.1, 2009.

Escamilla, J. A., Comerford, N. B., and Neary, D. G., Soil-Core Break Method to Estimate Pine Root Distribution, Soil Sci. Soc. Am. J., 55, 1722–1726, https://doi.org/10.2136/sssaj1991.03615995005500060036x, 1991.

European Union - SOeS: CORINE Land Cover, 2018.

Ferretti, F., Saltelli, A., and Tarantola, S., Trends in sensitivity analysis practice in the last decade. Science of The Total Environment 568, 666–670. https://doi.org/10.1016/j.scitotenv.2016.02.133, 2016

Fisher, R.A., and Koven, C.D., Perspectives on the Future of Land Surface Models and the Challenges of Representing Complex Terrestrial Systems. J Adv Model Earth Syst 12, e2018MS001453. https://doi.org/10.1029/2018MS001453, 2020.

Freeling, M. and Walbot, V. (Eds.), The Maize Handbook, Springer New York, New York, NY, https://doi.org/10.1007/978-1-4612-2694-9, 1994.

Friesen, J., and Van Stan, J.T., Early European Observations of Precipitation Partitioning by Vegetation: A Synthesis and Evaluation of 19th Century Findings, Geosciences, 9, 423, https://doi.org/10.3390/geosciences9100423, 2019.

Gowdy, M., Pieri, P., Suter, B., Marguerit, E., Destrac-Irvine, A., Gambetta, G., and van Leeuwen, C.: Estimating Bulk Stomatal Conductance in Grapevine Canopies, Front. Plant Sci., 13, https://doi.org/10.3389/fpls.2022.839378, 2022.

Grassland: Mission: Biomes: https://earthobservatory.nasa.gov/biome/biograssland.php, last access: 30 May 2023.

Habets, F., Boone, A., Champeaux, J. L., Etchevers, P., Franchistéguy, L., Leblois, E., Ledoux, E., Le Moigne, P., Martin, E., Morel, S., Noilhan, J., Quintana Seguí, P., Rousset-Regimbeau, F., and Viennot, P.: The SAFRAN-ISBA-MODCOU hydrometeorological model applied over France, J. Geophys. Res., 113, D06113, https://doi.org/10.1029/2007JD008548, 2008.

Hogue, Terri S., Luis A. Bastidas, Hoshin V. Gupta, and Sorooshian, S., Evaluating Model Performance and Parameter Behavior for Varying Levels of Land Surface Model Complexity. Water Resources Research, 42, 8. https://doi.org/10.1029/2005WR004440, 2006.

Hovenden, M. J. and Brodribb, T., Altitude of origin influences stomatal conductance and therefore maximum assimilation rate in Southern Beech, Nothofagus cunninghamii, Funct. Plant Biol., 27, 451, https://doi.org/10.1071/PP99164, 2000.

IUSS Working Group WRB, World Reference Base for Soil Resources. International soil classification system for naming soils and creating legends for soil maps, 4th edition., International Union of Soil Sciences (IUSS), Vienna, Austria, 2022.

Jarvis, P. G., The Interpretation of the Variations in Leaf Water Potential and Stomatal Conductance Found in Canopies in the Field, Philos. Trans. R. Soc. Lond. B. Biol. Sci., 273, 593–610, 1976.

Jeannot, B., Weill, S., Eschbach, D., Schmitt, L., and Delay, F., A Low-Dimensional Integrated Subsurface Hydrological Model Coupled with 2-D Overland Flow: Application to a Restored Fluvial Hydrosystem (Upper Rhine River – France), Journal of Hydrology, 563, 495-509. https://doi.org/10.1016/j.jhydrol.2018.06.028, 2018.

Jing Y., Liu, Y., Yang, W. and Chen, Y., Multi-Objective Sensitivity Analysis of a Fully Distributed Hydrologic Model WetSpa ». Water Resources Management 26, 1, 109-128, https://doi.org/10.1007/s11269-011-9908-9, 2012.

Jonard, F., André, F., Ponette, Q., Vincke, C., and Jonard, M., Sap flux density and stomatal conductance of European beech and common oak trees in pure and mixed stands during the Summer drought of 2003, J. Hydrol., 409, 371–381, https://doi.org/10.1016/j.jhydrol.2011.08.032, 2011.

Ju, J., Dai, H., Wu, C., Hu, B., Ye, M., Chen, X., Gui, D., Liu, H., and Zhang, J., Quantifying the Uncertainty of the Future Hydrological Impacts of Climate Change: Comparative Analysis of an Advanced Hierarchical Sensitivity in Humid and Semiarid Basins. Journal of Hydrometeor., 22, 601-621. https://doi.org/10.1175/JHM-D-20-0016.1, 2021.

https://doi.org/10.5194/hess-2024-73
Preprint. Discussion started: 4 April 2024

Kergoat, L., A model for hydrological equilibrium of leaf area index on a global scale, J. Hydrol., 212–213, 268–286, https://doi.org/10.1016/S0022-1694(98)00211-X, 1998.

Kim, J. and Verma, S. B., Modeling canopy stomatal conductance in a temperate grassland ecosystem, Agric. For. Meteorol., 55, 149–166, https://doi.org/10.1016/0168-1923(91)90028-O, 1991.

Kustas, W. P. and Daughtry, C. S. T., Estimation of the soil heat flux/net radiation ratio from spectral data, Agric. For. Meteorol., 49, 205–223, https://doi.org/10.1016/0168-1923(90)90033-3, 1990.

Lawrence, D.M., Fisher, R.A., Koven, C.D., Oleson, K.W., Swenson, S.C., Bonan, G., Collier, N., Ghimire, B., van Kampenhout, L., Kennedy, D., Kluzek, E., Lawrence, P.J., Li, F., Li, H., Lombardozzi, D., Riley, W.J., Sacks, W.J., Shi, M., Vertenstein, M., Wieder, W.R., Xu, C., Ali, A.A., Badger, A.M., Bisht, G., van den Broeke, M., Brunke, M.A., Burns, S.P., Buzan, J., Clark, M., Craig, A., Dahlin, K., Drewniak, B., B. Fisher, J.B., Flanner, M., Fox, A.M., Gentine, P., Hoffman, F., Keppel-Aleks, G., Knox, R., Kumar, S., Lenaerts, J., Leung, L.R., Lipscomb, W.H., Lu, Y., Pandey, A., Pelletier, J.D., Perket, J., Randerson, J.T., Ricciuto, D.M., Sanderson, B.M., Slater, A., Subin, Z.M., Tang, J., Thomas, R.Q., Val Martin, M., Zeng., X., The Community Land Model Version 5: Description of New Features, Benchmarking, and Impact of Forcing Uncertainty. Journal of Advances in Modeling Earth Systems 11, 12, 4245-4287. https://doi.org/10.1029/2018MS001583, 2019.

Leuschner, C., Hertel, D., Coners, H., and Büttner, V., Root competition between beech and oak: a hypothesis, Oecologia, 126, 276–284, https://doi.org/10.1007/s004420000507, 2001.

Li, J., Duan, Q. Y., Gong, W., Ye, A., Dai,Y., Miao, C., Di, Z., Tong, C., and Sun, Y., Assessing Parameter Importance of the Common Land Model Based on Qualitative and Quantitative Sensitivity Analysis, Hydrology and Earth System Sciences 17, 3279-3293. https://doi.org/10.5194/hess-17-3279-2013, 2013.

Liang, X., and Guo, J., Intercomparison of Land-Surface Parameterization Schemes: Sensitivity of Surface Energy and Water Fluxes to Model Parameters. Journal of Hydrology 279, 1-4, 182-209. https://doi.org/10.1016/S0022-1694(03)00168-9, 2003.

Liu, J., Skidmore, A. K., Wang, T., Zhu, X., Premier, J., Heurich, M., Beudert, B., and Jones, S., Variation of leaf angle distribution quantified by terrestrial LiDAR in natural European beech forest, ISPRS J. Photogramm. Remote Sens., 148, 208–220, https://doi.org/10.1016/j.isprsjprs.2019.01.005, 2019.

McCuen, R.H., The role of sensitivity analysis in hydrologic modeling. Journal of Hydrology 18, 37–53. https://doi.org/10.1016/0022-1694(73)90024-3, 1973.

https://doi.org/10.5194/hess-2024-73
Preprint. Discussion started: 4 April 2024

Mahhou, A., DeJong, T. M., Cao, T., and Shackel, K. S., Water stress and crop load effects on vegetative and fruit growth of 'Elegant Lady' peach [Prunus persica (L.) Batch] trees, Fruits, 60, 55–68, https://doi.org/10.1051/fruits:2005013, 2005.

Mai, J., Craig, J. R., Tolson, B. A., and Arsenault, R., The sensitivity of simulated streamflow to individual hydrologic processes across North America. *Nature Communications*, *13*(1), 455. https://doi.org/10.1038/s41467-022-28010-7, 2022.

Maina, F. Z., and Guadagnini, A., Uncertainty Quantification and Global Sensitivity Analysis of Subsurface Flow Parameters to Gravimetric Variations during Pumping Tests in Unconfined Aquifers. Water Resources Research, 54(1), 501-518. https://doi.org/10.1002/2017WR021655, 2018.

Maina, F. Z., Siirila-Woodburn, E.R., and Dennedy-Frank, P.J., Assessing the Impacts of Hydrodynamic Parameter Uncertainties on Simulated Evapotranspiration in a Mountainous Watershed. Journal of Hydrology, 08, 127620, https://doi.org/10.1016/j.jhydrol.2022.127620, 2022.

Maneta, M. P., and Silverman, N.L., A Spatially Distributed Model to Simulate Water, Energy, and Vegetation Dynamics Using Information from Regional Climate Models ». Earth Interactions 17, 11, 1-44. https://doi.org/10.1175/2012EI000472.1, 2013.

Manabe, S., Climate and the ocean circulation. I. The atmospheric circulation and the hydrology of the earth's surface. Monthly Weather Review, 97, 11, 739-774, https://doi.org/10.1175/1520-0493(1969)097<0739:CATOC>2.3.CO;2 1969.

Matese, A., Di Gennaro, S. F., and Berton, A., Assessment of a canopy height model (CHM) in a vineyard using UAV-based multispectral imaging, Int. J. Remote Sens., 38, 2150–2160, https://doi.org/10.1080/01431161.2016.1226002, 2017.

Mueller, K. E., Tilman, D., Fornara, D. A., and Hobbie, S. E.: Root depth distribution and the diversity–productivity relationship in a long-term grassland experiment, Ecology, 94, 787–793, https://doi.org/10.1890/12-1399.1, 2013.

Neitsch, S.L., Arnold, J.G., Kiniry, J.R., Williams, J.R., and King., K.W., Soil and Water Assessment Tool (SWAT) User's Manual, Version 2000, Grassland Soil and Water Research Laboratory. Blackland Research Center, Texas Agricultural Experiment Station, Texas Water Resources Institute, Texas Water Resources Institute, College Station, Texas, 2002.

https://doi.org/10.5194/hess-2024-73
Preprint. Discussion started: 4 April 2024

Niu, G-Y., Yang, Z-L., Mitchell, K.E., Chen, F., Ek, M.B., Barlage, M., Kumar, A., Manning, K., Niyogi, D., Rosero, E., Tewari, M., and Xia, Y., The Community Noah Land Surface Model with Multiparameterization Options (Noah-MP): 1. Model Description and Evaluation with Local-Scale Measurements, Journal of Geophysical Research: Atmospheres, 116, D12. https://doi.org/10.1029/2010JD015139, 2011.

Nicholas, K. A., Matthews, M. A., Lobell, D. B., Willits, N. H., and Field, C. B., Effect of vineyard-scale climate variability on Pinot noir phenolic composition, Agric. For. Meteorol., 151, 1556–1567, https://doi.org/10.1016/j.agrformet.2011.06.010, 2011.

Norman, J.M., Kustas, W.P., and Humes,. K.S., Source Approach for Estimating Soil and Vegetation Energy Fluxes in Observations of Directional Radiometric Surface Temperature, Agricultural and Forest Meteorology 77, 3-4, 263-293, https://doi.org/10.1016/0168-1923(95)02265-Y, 1995.

Ocheltree, T. W., Nippert, J. B., and Prasad, P. V. V., Changes in stomatal conductance along grass blades reflect changes in leaf structure: Changes in stomatal conductance along grass blades, Plant Cell Environ., 35, 1040–1049, https://doi.org/10.1111/j.1365-3040.2011.02470.x, 2012.

Overgaard, J., Rosbjerg, D., Butts, M.B., Land-surface modelling in hydrological perspective – a review, Biogeosciences, 3, 229–241, https://doi.org/10.5194/bg-3-229-2006, 2006.

Pan, Yi, Weill, S., Ackerer, P., and Delay., F., A Coupled Stream Flow and Depth-Integrated Subsurface Flow Model for Catchment Hydrology. Journal of Hydrology, 530, 66-78. https://doi.org/10.1016/j.jhydrol.2015.09.044, 2015.

Peel, M. C., Finlayson, B. L., and Mcmahon, T. A., Updated world map of the Köppen-Geiger climate classification, Hydrology and Earth System Sciences, 11, 5, 1633-1644, https://doi.org/10.5194/hess-11-1633-2007, 2007.

Peiffer, J. A., Romay, M. C., Gore, M. A., Flint-Garcia, S. A., Zhang, Z., Millard, M. J., Gardner, C. A. C., McMullen, M. D., Holland, J. B., Bradbury, P. J., and Buckler, E. S., The Genetic Architecture Of Maize Height, Genetics, 196, 1337–1356, https://doi.org/10.1534/genetics.113.159152, 2014.

Quintana-Seguí, P., Le Moigne, P., Durand, Y., Martin, E., Habets, F., Baillon, M., Canellas, C., Franchisteguy, L., and Morel, S., Analysis of Near-Surface Atmospheric Variables: Validation of the SAFRAN Analysis over France, J. Appl. Meteorol. Climatol., 47, 92–107, https://doi.org/10.1175/2007JAMC1636.1, 2008.

Razavi, S., Jakeman, A., Saltelli, A., Prieur, C., Iooss, B., Borgonovo, E., Plischke, E., Lo Piano, S., Iwanaga, T., Becker, W., Tarantola, S., Guillaume, J.H.A., Jakeman, J., Gupta, H., Melillo, N., Rabitti,

https://doi.org/10.5194/hess-2024-73
Preprint. Discussion started: 4 April 2024

Hydrology and Earth System Sciences Discussions

G., Chabridon, V., Duan, Q., Sun, X., Smith, S., Sheikholeslami, R., Hosseini, N., Asadzadeh, M., Puy, A., Kucherenko, S., Maier, H.R., The Future of Sensitivity Analysis: An essential discipline for systems modeling and policy support. Environmental Modelling & Software 137, 104954. https://doi.org/10.1016/j.envsoft.2020.104954, 2021.

Reis, M. G. D. and Ribeiro, A.:, Conversion factors and general equations applied in agricultural and forest meteorology, Agrometeoros, 27, https://doi.org/10.31062/agrom.v27i2.26527, 2020.

Richards, D., The Grape Root System, in: Horticultural Reviews, edited by: Janick, J., John Wiley & Sons, Inc., Hoboken, NJ, USA, 127–168, https://doi.org/10.1002/9781118060728.ch3, 2011.

Saltelli, A., Ed. Sensitivity Analysis in Practice: A Guide to Assessing Scientific Models. Reprinted. Chichester Weinheim: Wiley, 2007.

Sandoval, L., Riva, M., Colombo, I., and Guadagnini, A., Sensitivity Analysis and Quantification of the Role of Governing Transport Mechanisms and Parameters in a Gas Flow Model for Low-Permeability Porous Media. Transport in Porous Media, 142, 3, 509-530, https://doi.org/10.1007/s11242-022-01755-x, 2022.

Seibert, J., and Vis, M. J. P, Teaching Hydrological Modeling with a User-Friendly Catchment-Runoff-Model Software Package ». Hydrology and Earth System Sciences 16, 9, 3315-3325. https://doi.org/10.5194/hess-16-3315-2012, 2012.

Seibert, J., and Bergström, S.A Retrospective on Hydrological Catchment Modelling Based on Half a Century with the HBV Model ». Hydrology and Earth System Sciences 26, 5, 1371-1388. https://doi.org/10.5194/hess-26-1371-2022, 2022.

Singh, R. K. and Sharma, R. V., Numerical analysis for ground temperature variation, Geotherm. Energy, 5, 22, https://doi.org/10.1186/s40517-017-0082-z, 2017.

Smirnova, E., Bergeron, Y., Brais, S., and Granström, A. Postfire root distribution of Scots pine in relation to fire behaviour, Can. J. For. Res., 38, 353–362, https://doi.org/10.1139/X07-127, 2008.

Sobol, I. M., Global sensitivity indices for nonlinear mathematical models and their Monte Carlo estimates, Math. Comput. Simul., 55, 271–280, https://doi.org/10.1016/S0378-4754(00)00270-6, 2001.

https://doi.org/10.5194/hess-2024-73
Preprint. Discussion started: 4 April 2024

Hydrology and Earth System Sciences
Discussions

Song, X., Zhang, J., Zhan, C., Xuan, Y., Ye, M., and Xu, C. Global sensitivity analysis in hydrological modeling: Review of concepts, methods, theoretical framework, and applications, Journal of Hydrology, 523, 739–757, https://doi.org/10.1016/j.jhydrol.2015.02.013, 2015.

Song, X., Gao, X., Dyck, M., Zhang, W., Wu, P., Yao, J., and Zhao, X., Soil water and root distribution of apple tree (Malus pumila Mill) stands in relation to stand age and rainwater collection and infiltration system (RWCI) in a hilly region of the Loess Plateau, China, CATENA, 170, 324–334, https://doi.org/10.1016/j.catena.2018.06.026, 2018.

Taconet, O., Bernard, R., and Vidal-Madjar, D., Evapotranspiration over an Agricultural Region Using a Surface Flux/Temperature Model Based on NOAA-AVHRR Data, J. Clim. Appl. Meteorol., 25, 284–307, https://doi.org/10.1175/1520-0450(1986)025<0284:EOAARU>2.0.CO;2, 1986.

Tardieu, F., Katerji, N., Bethenod, O., Zhang, J., and Davies, W. J., Maize stomatal conductance in the field: its relationship with soil and plant water potentials, mechanical constraints and ABA concentration in the xylem sap, Plant Cell Environ., 14, 121–126, https://doi.org/10.1111/j.1365-3040.1991.tb01378.x, 1991.

van Dam, J.C., Groenendijk, P., Hendriks, R.F.A. and Kroes, J.G. Advances of Modeling Water Flow in Variably Saturated Soils with SWAP. Vadose Zone Journal, 7, 640-653, https://doi.org/10.2136/vzj2007.0060, 2008.

Vemuri, V., Dracup, J.A., Erdmann, R.C. and Vemuri, N., Sensitivity Analysis Method of System Identification and Its Potential in Hydrologic Research. Water Resources Research 5, 2, 341-349, https://doi.org/10.1029/WR005i002p00341, 1969.

Vidal, J.-P., Martin, E., Franchistéguy, L., Baillon, M., and Soubeyroux, J.-M., A 50-year high-resolution atmospheric reanalysis over France with the Safran system, Int. J. Climatol., 30, 1627–1644, https://doi.org/10.1002/joc.2003, 2010.

Wiltshire, A. J., Rojas, C. D., Edwards, J., Gedney, N., Harper, A. B., Hartley, A., Hendry, M. A., Robertson, E., and Smout-Day, K., JULES-GL7: The global land configuration of the joint UK land environment simulation version 7.0. Geoscientific Model Development Discussion. https://doi.org/10.5194/gmd-2019-152, 2019.

Winkel, T. and Rambal, S., Influence of Water Stress on Grapevines Growing in the Field: From Leaf to Whole-Plant Response, Funct. Plant Biol., 20, 143, https://doi.org/10.1071/PP9930143, 1993.

Yokohata, T., Kinoshita, T., Sakurai, G., Pokhrel, Y., Ito, A., Okada, M., Satoh, Y., Kato, E., Nitta, T., Fujimori, S., Felfelani, F., Masaki, Y., Iizumi, T., Nishimori, M., Hanasaki, N., Takahashi, K.,

https://doi.org/10.5194/hess-2024-73
Preprint. Discussion started: 4 April 2024

Hydrology and Earth System Sciences Discussions

Yamagata, Y., and Emori, S., MIROC-INTEG1: A global bio-geochemical land surface model with human water management, crop growth, and land-use change. Geoscientific Model Development Discussion. https://doi.org/10.5194/gmd-2019-184, 2019.

Zeighami, F., Sandoval, L., Guadagnini A., and Di Federico, V., Uncertainty quantification and global sensitivity analysis of seismic metabarriers, Engineering Structures, 277, 115415, 1-13, https://doi.org/10.1016/j.engstruct.2022.115415, 2023.

Zhang, L., Hu, Z., Fan, J., Zhou, D., and Tang, F., A meta-analysis of the canopy light extinction coefficient in terrestrial ecosystems, Front. Earth Sci., 8, 599–609, https://doi.org/10.1007/s11707-014-0446-7, 2014.

Zhang, Y., Oren, R., and Kang, S., Spatiotemporal variation of crown-scale stomatal conductance in an arid Vitis vinifera L. cv. Merlot vineyard: direct effects of hydraulic properties and indirect effects of canopy leaf area, Tree Physiol., 32, 262–279, https://doi.org/10.1093/treephys/tpr120, 2012.